

Bayesian clustering of high-dimensional data

Noirrit Kiran Chandra*, Antonio Canale[†] and David B. Dunson[‡]

Abstract

In many applications, it is of interest to cluster subjects based on very high-dimensional data. Although Bayesian discrete mixture models are often successful at model-based clustering, we demonstrate pitfalls in high-dimensional settings. The first key problem is a tendency for posterior sampling algorithms based on Markov chain Monte Carlo to produce a very large number of clusters that slowly decreases as sampling proceeds, indicating serious mixing problems. The second key problem is that the true posterior also has aberrant behavior but potentially in the opposite direction. In particular, we show that, for diverging dimension and fixed sample size, the true posterior either assigns each observation to a different cluster or all observations to the same cluster, depending on the kernels and prior specification. We propose a general strategy for solving these problems by basing clustering on a discrete mixture model for a low-dimensional latent variable. We refer to this class of methods as LATent Mixtures for Bayesian (Lamb) clustering. Theoretical support is provided, and we illustrate substantial gains relative to clustering on the observed data level in simulation studies. The methods are motivated by an application to clustering of single cell RNAseq data, with the clusters corresponding to different cell types.

Keywords: Big data; Clustering; Dirichlet process; Exchangeable partition probability function; Latent variables; Mixture model; Pitman–Yor process.

*Department of Statistical Science, Duke University, Durham, NC noirritchandra@gmail.com

[†]Dipartimento di Scienze Statistiche, Università degli Studi di Padova, Padova, Italy canale@stat.unipd.it

[‡]Departments of Statistical Science and Mathematics, Duke University, Durham, NC dunson@duke.edu

1. INTRODUCTION

It has become a cliché that, in modern applications, it is routine to collect high-dimensional data $y_i = (y_{i1}, \dots, y_{ip})^T$ for $i = 1, \dots, n$, with p (dimension of the data) being larger than the sample size n . In such settings, it is very common to be interested in clustering subjects. For example, for individual patients, suppose we have data consisting of a variety of high-dimensional *biomarkers* (e.g., gene expression, metabolomics, etc). Then, it is often of interest to identify subgroups of patients that have different biomarker profiles. In this setting, $p \gg n$ and one can conceptually increase p to arbitrarily huge values by including multiple types of omics data, monitor information, etc.

We are particularly motivated by the analysis of single-cell RNA sequencing (scRNASeq) data and its application to the study of cancer. Single cell sequencing can be very useful in disentangling carcinogenic processes. Tumors are formed by cancer cells and by many non-cancerous cell types forming the tumor microenvironment. Transcriptome analyses have been widely used to segregate different tumor types, classifying them into subtypes to predict response to therapy and patient outcomes. However, the classification of different cell types and especially the identification of rare populations has been limited in bulk RNAseq transcriptomic analyses. Single-cell RNAseq analysis has emerged as a powerful method to unravel the heterogeneity between different cell types. It has also been established to be very useful in the study of rare cell populations, especially in cancer (Valdes-Mora et al. 2018). From the statistical standpoint, the identification of different cell populations is obtained by means of suitable clustering techniques.

In general, there are two main approaches for clustering — distance- and model-based methods. Distance-based approaches require choice of a distance metric between pairs of data points, $d(y, y')$; for continuous measurements, by far the most common choice is the Euclidean distance. However, for very large p , problems arise in using Euclidean distance, motivating a literature on dimensionality reduction approaches. For example, prior to conducting clustering, it is common to apply first stage dimensionality reduction, such as principal components analysis (PCA) or sparse PCA (Zou et al. 2006). Subsequently one can cluster in a lower-dimensional space. Such two stage approaches can work reasonably well, particularly when many of the measured variables are redundant and highly correlated with each other. However, there are some clear drawbacks. Firstly, the dominant principal components may not be those most related to distinct clusters in the data, so that clusters may be obscured by applying usual PCA in a first stage without taking into account that clustering is the goal. Also, this type of approach simply

produces one best guess at a clustering in the data; in reality, there is substantial uncertainty that should be taken into account in performing inferences. A primary advantage of model-based Bayesian approaches is their ability to characterize such uncertainty.

The model-based framework for clustering is based on the mixture model

$$y_i \sim f, \quad f(y) = \sum_{h=1}^k \pi_h \mathcal{K}(y; \theta_h), \quad (1)$$

where k is the number of clusters, $\pi = (\pi_1, \dots, \pi_k)^T$ is a vector of probability weights on the different clusters, and $\mathcal{K}(y; \theta_h)$ characterizes the density of the data within cluster h . When p is large and $y_i \in \mathbb{R}^p$, a typical approach is to choose $\mathcal{K}(y; \theta_h)$ as a multivariate Gaussian density with a constrained and parsimonious representation of the covariance matrix (see Bouveyron and Brunet-Saumard 2014, for a review). Examples include matrices that are diagonal (Banfield and Raftery 1993; Celeux and Govaert 1995), block diagonal (Galimberti and Soffritti 2013) or have a factor analytic representation (Ghahramani et al. 1996).

In practice, the true number of clusters is typically unknown, and hence data are used to select a good value. In frequentist inference, model (1) is typically fitted with the EM algorithm for varying k and then AIC, BIC or another criterion is used to choose k . In the Bayesian literature, there is a rich variety of approaches to account for uncertainty in k . Richardson and Green (1997) proposed to choose a prior on k , and then update it along with the other parameters using reversible jump (RJ) Markov chain Monte Carlo (MCMC). Although RJ-MCMC can be very inefficient, Miller and Harrison (2018) recently proposed improved computational algorithms for inference under such mixture of finite mixture models. A disadvantage of this type approach is that it assumes the number of clusters k does not depend on the sample size n , while it is typically more natural to suppose that new clusters can be discovered at a slow rate as n increases. This motivates a Bayesian nonparametric approach that lets $k = \infty$, with the number of non-empty clusters in a sample of size n denoted as $k_n \leq n$. Under a Dirichlet process (Ferguson 1973) k_n increases as a log rate in n , while for a Pitman-Yor process (Pitman and Yor 1997) the rate is a power law.

However, when p is very large, problems arise in following these approaches. In many applications, it has been noticed that the posterior distribution of k_n has a tendency to concentrated on large values (Celeux et al. 2018); often the posterior mode of k_n is even equal to n so that each subject is assigned to its own singleton cluster. This type of behavior is highly undesirable,

as the whole point of clustering is to obtain a small number of groups of relatively distinct subjects. Celeux et al. (2018) conjecture that this aberrant behavior is mainly due to slow mixing of MCMC samplers. In our experiments, we noticed a tendency for MCMC to initially produce a large number of clusters (approaching n) that is then very slowly reduced as the sampler proceeds. This occurred even if the true number of clusters was small. Frühwirth-Schnatter (2006) propose a specific prior elicitation criterion (the so called determinant method) to combat this issue. Although this has been successful in a variety of situations with moderate dimension p (in the order of hundreds), calibration of prior parameters remains a delicate issue and scaling to high dimensions (above several thousands) is problematic.

It is important to disentangle the clustering properties of the true posterior from the behavior observed empirically based on MCMC samples. We provide theory showing that, as $p \rightarrow \infty$ with n fixed, the true posterior tends to assign probability one to a trivial clustering - either with $k_n = 1$ and all subjects in one cluster or with $k_n = n$ and every subject in a different cluster. A related result was shown by Bickel and Levina (2004) in a classification context; they showed that when p increases at a faster rate than n , the Fisher’s linear discriminant rule is equivalent to randomly assigning future observations to the existing classes.

There is an existing literature on clustering of high-dimensional data, which attempts to address some of the issues mentioned above. One appealing approach is variable selection in clustering (Tadesse et al. 2005), which is based on the idea that it is only appropriate to cluster subjects based on a subset of the variables in y_i , with this subset unknown and estimated based on the data. Kim et al. (2006) combine Dirichlet process mixtures (Escobar and West 1995, DPMs) with variable selection priors (George and McCulloch 1993), developing an MCMC algorithm for posterior computation. A related approach is to introduce both global and local (variable-specific) clustering indices for each subject, so that only certain variables inform about their global cluster allocation (Dunson 2009). Alternatively, if the high-dimensional variables correspond to sets of observations in different domains, one can suppose that domain-specific clustering is an error-prone realization of global clustering indices. This leads to a notion of consensus clustering (Lock and Dunson 2013).

We propose a fundamentally different approach we refer to as LATent Mixtures for Bayesian (Lamb) clustering. Our idea is motivated by modern medical contexts in which there is essentially no limit to the number of measurements that we can take on a patient. However, in these measurements there is a lot of redundant information and noise with the intrinsic dimension

being much smaller. Consistently with this assumption, we propose a modification of model (1) which assumes a mixture model for unobserved d -dimensional latent factors η_i with $d \ll p$ and defines a suitable p -dimensional distribution of the observed data y_i conditionally on these η_i .

1.1 Notation and summary of the paper

We denote by $\|x\|$ the Euclidean norm of a vector x and by $\|X\|_2$ the spectral norm of a matrix X . $s_{\min}(X)$ and $s_{\max}(X)$ denotes the smallest and largest eigen values of the matrix $(X^T X)^{\frac{1}{2}}$ respectively. For a positive-definite matrix X , $\lambda_{\min}(X)$ and $\lambda_{\max}(X)$ denotes the smallest and largest eigenvalues respectively. $\mathcal{N}_r(\cdot; \mu, \Sigma)$ denotes the r -dimensional multivariate normal density with mean μ and dispersion matrix Σ .

Section 2 gives details on the limiting behavior of usual clustering methods based on (1). Section 3 introduces our Lamb approach, studies limiting behavior, and considers applications. In Section 4 we show that Lamb attains a Bayesian oracle clustering rule asymptotically. In Section 5 we describe a posterior sampling algorithm for implementing Lamb. Section 6 contains simulation studies comparing Lamb with some popular clustering methods. Section 7 illustrates the method with an application to scRNASeq data, and Section 8 discusses the results. Proofs of the main results are included in an Appendix, while additional simulation results and theorems along with proofs are in a Supplement.

2. LIMITING BEHAVIOR OF HIGH-DIMENSIONAL MODEL-BASED CLUSTERING

Under a Bayesian nonparametric framework, rewrite model (1) as

$$f(y) = \int \mathcal{K}(y; \theta) dP(\theta), \quad (2)$$

where $P \sim PY(\alpha, \sigma, P_0)$ is a random nonparametric mixing distribution with $PY(\alpha, \sigma, P_0)$ denoting the Pitman-Yor process with strength and discount parameters α and σ , respectively, and base measure P_0 . When $\sigma = 0$ we obtain the Dirichlet process.

Let $c_i \in \{1, \dots, \infty\}$ denote the cluster label for subject i (for $i = 1, \dots, n$), with $k = \#\{c_1, \dots, c_n\}$ denoting the number of clusters represented in the sample. Conditionally on $c_i = h$, we can write $y_i \mid c_i = h \sim \mathcal{K}(y_i; \theta_h)$. Assume that n_j is the size of the j th cluster with $\sum_{j=1}^{k_n} n_j = n$. The posterior probability of observing the partition Ψ induced by the clusters

c_1, \dots, c_n conditionally on the data $\mathbf{y} = (y_1, \dots, y_n)^T$ is

$$\Pi(\Psi \mid \mathbf{y}) = \frac{\Pi(\Psi) \times \prod_{h \geq 1} \int \prod_{i: c_i = h} \mathcal{K}(y_i; \theta) dP_0(\theta)}{\sum_{\Psi' \in \mathcal{P}} \Pi(\Psi') \times \prod_{h \geq 1} \int \prod_{i: c_i = h} \mathcal{K}(y_i; \theta) dP_0(\theta)}. \quad (3)$$

The numerator of (3) is the product of the prior probability of Ψ multiplied by the likelihood of \mathbf{y} conditionally on the cluster allocations, which can be expressed as a product of marginal likelihoods for the observations in each cluster. The denominator is then a normalizing constant consisting of an enormous sum over \mathcal{P} , the space of all possible partitions of n data into clusters. For Pitman-Yor and other Gibbs-type priors for P in (2), P can be marginalized out to obtain a closed form analytic expression for the prior probability of any partition of n subjects into k groups. This prior probability just depends on the cluster sizes $n_j, j = 1, \dots, k$, and number of clusters k through what is known as the exchangeable partition probability function (EPPF).

The posterior (3) forms the basis for Bayesian inferences on clusterings in the data, while providing a characterization of uncertainty. We are particularly interested in how this posterior behaves in the case in which $y_i = (y_{i1}, \dots, y_{ip})'$ are high-dimensional so that p is very large. To study this behavior theoretically, we consider the limiting case as $p \rightarrow \infty$ while keeping n fixed. This asymptotic setting is quite appropriate in our motivating applications to genomics and precision medicine, as there is essentially no limit in the number of variables one can measure on each study subject, while the number of study subjects is often quite modest.

In such settings with enormous p and modest n , we would ideally like the true posterior distribution in (3) to provide a realistic characterization of potential clusters in the data. In fact, we find that this is not the case, and as p increases the posterior distribution on clusterings has one of two trivial degenerate limits. In particular, depending on the true data-generating density f_0 and the choice of \mathcal{K} and P_0 in (2), the posterior assigns probability one to either the $k = 1$ clustering that places all subjects in the same cluster or the $k = n$ clustering that places all subjects in different clusters. This result is formalized in the following theorem.

Theorem 1. *Let y_1, \dots, y_n denote iid draws from p -variate continuous density f_0 . Let Ψ denote the partition induced by the cluster labels c_1, \dots, c_n , and let c'_1, \dots, c'_n denote a new set of cluster labels obtained from c_1, \dots, c_n by merging an arbitrary pair of clusters, with Ψ' the related partition. If*

$$\limsup_{p \rightarrow \infty} \frac{\prod_{h \geq 1} \int \prod_{i: c_i = h} \mathcal{K}(y_i; \theta) dP_0(\theta)}{\prod_{h \geq 1} \int \prod_{i: c'_i = h} \mathcal{K}(y_i; \theta) dP_0(\theta)} = 0 \text{ in } f_0\text{-probability,}$$

then $\lim_{p \rightarrow \infty} \Pi(c_1 = \dots = c_n \mid \mathbf{y}) = 1$. Else if

$$\liminf_{p \rightarrow \infty} \frac{\prod_{h \geq 1} \int \prod_{i: c_i = h} \mathcal{K}(y_i; \theta) dP_0(\theta)}{\prod_{h \geq 1} \int \prod_{i: c'_i = h} \mathcal{K}(y_i; \theta) dP_0(\theta)} = \infty \text{ in } f_0\text{-probability,}$$

then $\lim_{p \rightarrow \infty} \Pi(c_1 \neq \dots \neq c_n \mid \mathbf{y}) = 1$.

Theorem 1 has disturbing implications in terms of the behavior of posterior distributions for Bayesian clustering in large p settings. To obtain insight into this result, we consider an important special case corresponding to a nonparametric location mixture of multivariate Gaussian kernels:

$$y_i \stackrel{\text{iid}}{\sim} f, \quad f(y) = \sum_{h=1}^{\infty} \pi_h \mathcal{N}_p(y; \xi_h, \Sigma), \quad \xi_h \mid \Sigma \stackrel{\text{iid}}{\sim} P_{\xi \mid \Sigma}, \quad \Sigma \sim P_{\Sigma}, \quad (4)$$

where $P_{\xi \mid \Sigma}$ and P_{Σ} are suitable prior base measures on the kernel's parameters. By assuming the covariance Σ is fixed across components, we dramatically reduce the number of parameters under the assumption that the clusters all have the same shapes but with a shift in mean. A similar set-up has been considered in frequentist classification (Bickel and Levina 2004) and clustering (Cai et al. 2019) studies in high dimensions. To study the effect of over and under-parametrization, we consider two settings, respectively in Corollary 1 and 2.

Corollary 1. *Under model (4), assume $\Sigma = \sigma^2 I_p$ and $\xi_h = \mu_h \mathbf{1}_p$ where $\mathbf{1}_p$ is a p vector of ones. If $\|y_i\|^2 = O_p(p)$, $\mu_h \mid \sigma^2 \stackrel{\text{iid}}{\sim} \mathcal{N}(\mu_0, \kappa_0^{-1} \sigma^2)$, and $\sigma^2 \sim IG(\nu_0, \lambda_0)$, where $\mu_0, \kappa_0, \nu_0, \lambda_0$ are fixed hyperparameters, then $\Pi(c_1 \neq \dots \neq c_n \mid \mathbf{y}) \rightarrow 1$.*

Corollary 2. *Under model (4), assume $\xi_h = \mu_h$ with $\mu_h \in \mathbb{R}^p$. If $\|y_i\|^2 = O_p(p)$, $\mu_h \mid \Sigma \stackrel{\text{iid}}{\sim} \mathcal{N}_p(\mu_0, \kappa_0^{-1} \Sigma)$ and $\Sigma \sim IW(\nu_0, \Lambda_0)$, where $\mu_0, \kappa_0, \nu_0, \Lambda_0$ are the hyperparameters with $\nu_0 > p - 1$ and $\nu_0 = O(p)$, then $\Pi(c_1 = \dots = c_n \mid \mathbf{y}) \rightarrow 1$.*

Corollary 1 and 2 show that, for the same multivariate normal location mixture class and under the same weak assumption on the true data generating model, we can obtain directly opposite aberrant limiting behavior of the posterior depending on the prior. In the first case, covered by Corollary 1, we assume an overly-simplistic model structure in which all the mixture components are spherical with a single scalar times a unit vector for the mean. In the limiting case as $p \rightarrow \infty$, this model forces all individuals to be assigned to their own clusters with probability one regardless of the true data generating model f_0 . At the other extreme, Corollary

2 considers the case in which we allow the cluster-specific means to be flexible and the common covariance matrix to be flexible, under typical conjugate multivariate normal inverse Wishart priors. This case can be viewed as overly-complex as p increases, and to combat this complexity, the Bayesian Ockham razor (Jefferys and Berger 1992) automatically assigns probability one to grouping all n individuals into the same cluster, effectively simplifying the model.

These theoretical results demonstrate that in high dimensions it is crucial to choose a good compromise between parsimony and flexibility in Bayesian model-based clustering. Otherwise, the true posterior distribution of clusterings in the data can have effectively no relationship whatsoever with true clustering structure in the data. Although we focus on the limiting case as $p \rightarrow \infty$, we conjecture that the asymptotics of these results can ‘kick in’ quickly as p increases, based on intuition built through our proofs and through comprehensive simulation experiments. In the next section, we propose a happy medium between parsimony and flexibility that can solve these pitfalls .

3. LATENT FACTOR MIXTURE

To overcome the problems discussed in Section 2, we propose a general class of latent factor mixture models defined as

$$y_i \sim f(y_i; \eta_i, \psi), \quad \eta_i \sim \sum_{h=1}^{\infty} \pi_h \mathcal{K}(\eta_i; \theta_h), \quad (5)$$

where $\eta_i = (\eta_{i1}, \dots, \eta_{id})^T$ are d -dimensional latent variables, $d < n$ is fixed and not growing with p , $f(\cdot; \eta_i, \psi)$ is the density of the observed data conditional on the latent variables and measurement parameters ψ , and $\mathcal{K}(\cdot; \theta)$ is a d -dimensional kernel density.

Under (5), the high dimensional data being collected are assumed to provide error-prone measurements of an unobserved lower-dimensional set of latent variables η_i on subject i . As $p \rightarrow \infty$, we obtain more and more information on the latent variables η_i , so that the uncertainty in inferring them decreases to zero and they effectively become observed data. As η_i is d -dimensional, the information content of this variable is bounded, solving the pitfall discussed in Section 2.

As a canonical example, we focus on a linear Gaussian measurement model with a mixture

of Gaussians model for the latent factors:

$$y_i \sim \mathcal{N}_p(\Lambda \eta_i, \Sigma), \quad \eta_i \sim \sum_{h=1}^{\infty} \pi_h \mathcal{N}_d(\mu_h, \Delta_h), \quad (6)$$

where Σ is a $p \times p$ diagonal matrix and Λ is a $p \times d$ matrix of factor loadings. In order to accommodate very high-dimensional data, with $p \gg n$, it is important to reduce the effective number of parameters in the $p \times d$ loadings matrix Λ . There is a very rich literature on sparse factor modeling using a variety of shrinkage or sparsity priors for Λ ; for example, refer to Bhattacharya and Dunson (2011); Legramanti et al. (2020) and the references cited therein. Based on a simpler factor model that sets $\eta_i \sim \mathcal{N}_d(0, I)$, Pati et al. (2014) studied posterior concentration rates of the induced $p \times p$ covariance matrix of y_i in the high-dimensional setting. Although a wide variety of shrinkage priors for Λ are appropriate, we focus on a Dirichlet-Laplace prior (Bhattacharya et al. 2015), as it is convenient both computationally and theoretically. The resulting prior for Λ can be expressed in hierarchical form as

$$\lambda_{jh} | \phi, \tau \sim \text{DE}(\phi_{jh} \tau); \quad \text{vec}(\phi) \sim \text{Dir}(a, \dots, a); \quad \tau \sim \text{Ga}(pda, 1/2), \quad (7)$$

where λ_{jh} is the element in row j column h of the factor loading matrix Λ , $\text{DE}(a)$ is the double exponential or Laplace distribution with variance $2a^2$, $\text{Dir}(a_1, \dots, a_d)$ is the d -dimensional Dirichlet distribution, and $\text{Ga}(a, b)$ is the gamma distribution with mean a/b and variance a/b^2 .

To complete a specification of model (6), we require priors for the variances $\Sigma = \text{diag}(\sigma_1^2, \dots, \sigma_p^2)$, the weights $\{\pi_h\}$, and atoms $\{\mu_h, \Delta_h\}$. As a default, we choose inverse-Gamma priors for the residual variances: $\sigma_j^{-2} \stackrel{\text{iid}}{\sim} \text{Ga}(a_\sigma, b_\sigma)$, and use a nonparametric prior for the weights and atoms, such as the Pitman-Yor process with suitable base measure G_0 . Under model (6), we can marginalize out η_i to obtain an induced mixture on the observed data level, namely

$$y_i \sim \sum_{h=1}^{\infty} \pi_h \mathcal{N}_p(\Lambda \mu_h, \Lambda \Delta_h \Lambda^T + \Sigma). \quad (8)$$

Augmenting (8) with latent cluster indicator c_i , we obtain the conditional distributions

$$y_i \mid c_i = h \sim \mathcal{N}_p(\Lambda \mu_h, \Lambda \Delta_h \Lambda^T + \Sigma). \quad (9)$$

Expression (8) differs from the popular mixture of factor analyzers (Ghahramani et al. 1996)

in not having cluster-specific values for Λ and Σ . Based on our experience, we conjecture that usual mixtures of factor analyzers face the pitfall of Section 2, and to address this we fix both Λ and Σ across the mixture components, which massively reduces the number of parameters for huge p . We are effectively learning a common affine space within which we can define a simple location mixture of Gaussians. We find that (8) provides a successful compromise between the two extreme cases of Section 2.

We will consider three different special cases of the Lamb model in (8): (i) $\Delta_h = I_d$, (ii) $\Delta_h = \Delta$, and (iii) Δ_h varies flexibly across the components. In Section 4, we use the case (ii) model in defining a Bayesian oracle clustering rule, while showing that the posterior distribution under the case (i) Lamb model satisfies this oracle property and bypasses the pitfalls described in Section 2. In Section 5 we develop a posterior computation algorithm under the more flexible case (iii) model which is later used in Sections 6 and 7

4. PROPERTIES OF THE LAMB CLUSTERING METHOD

4.1 Bayes oracle clustering rule

In this section, we first define a Bayes oracle clustering rule. Cai et al. (2019) proposed an optimal frequentist clustering method in a related context, but focusing on the case in which there are exactly two clusters. To the best of our knowledge, there is no existing oracle for clustering with unknown number of clusters. We assume the oracle has knowledge of the exact values of the latent variables $\{\eta_{0i}\}$. Given this knowledge, the oracle can define a simple Bayesian location mixture model to induce a posterior clustering of the data, which is not affected by the high-dimensionality of the problem. We assume that the oracle uses a Pitman-Yor process location mixture with Gaussian base measure and independent Jeffreys' prior for the common covariance, i.e.

$$\eta_i \stackrel{\text{iid}}{\sim} \sum_{h=1}^{\infty} \pi_h \mathcal{N}_d(\mu_h, \Delta), \quad \mu_h | \Delta \stackrel{\text{iid}}{\sim} \mathcal{N}_d(0, \kappa_0^{-1} \Delta), \quad \Delta \propto |\Delta|^{-\frac{p+1}{2}}, \quad \pi_h \sim \text{Stick}_{\text{PY}}(\sigma, \alpha), \quad (10)$$

which leads to a distribution over the space of partitions defined in the following definition.

Definition 1. Let $\boldsymbol{\eta}_0 = (\eta_{01}, \dots, \eta_{0n})$ be the true values of the latent variables in model (10)

and Ψ be the partition induced by c_1, \dots, c_n . We define the Bayes oracle partition probability as

$$\Pi(\Psi \mid \boldsymbol{\eta}_0) = \frac{\Pi(\Psi) \times \int \prod_{h \geq 1} \prod_{i: c_i = h} \mathcal{K}(\eta_{0i}; \theta_h) dG_0(\theta)}{\sum_{\Psi' \in \mathcal{P}} \Pi(\Psi') \times \int \prod_{h \geq 1} \prod_{i: c'_i = h} \mathcal{K}(\eta_{0i}; \theta_h) dG_0(\theta)}. \quad (11)$$

Remark 1. Hereafter in this article we focus on the special case of the oracle rule under model (10), that is, where $\theta = \{\Delta, \mu_h; h \geq 1\}$; given $c_i = h$, $\mathcal{K}(\eta; \theta_h) = \mathcal{N}_d(\eta; \mu_h, \Delta)$ and $G_0(\theta) = \prod_{h \geq 1} \mathcal{N}_d(\mu_h; 0, \kappa_0^{-1} \Delta) \times |\Delta|^{-\frac{p+1}{2}}$. Note that for $d < n$ the oracle rule is well defined for the non-informative Jeffrey's prior on Δ .

Probability (11) expresses the oracles' uncertainty in clustering. This can be viewed as a gold standard uncertainty quantification in that it uses the oracles' knowledge of the true values of the latent variables, and hence is free of the curse of dimensionality that comes in as more and more variables are measured on each study subject. Under the Lamb framework of Section 3, the role of the high-dimensional measurements on each subject is to provide information on these latent variables, with the clustering done on the latent variable level. Ideally, we would get closer and closer to the oracle partition probability under the Lamb model as p increases, turning the curse of dimensionality into a blessing. We show that this is indeed the case in Section 4.2.

4.2 Main results

In this section, we show that the posterior probability on the space of partitions, induced by the case (i) Lamb model, converges to the oracle probability as $p \rightarrow \infty$. We assume the following conditions on the data generating process.

- (C1) $y_i \stackrel{\text{ind}}{\sim} \mathcal{N}_p(\Lambda_0 \eta_{0i}, \sigma_0^2 I_p)$, for each $i = 1, \dots, n$;
- (C2) $\lim_{p \rightarrow \infty} \left\| \frac{1}{p} \Lambda_0^T \Lambda_0 - v_0 I_d \right\|_2 = 0$ for some $v_0 > 0$;
- (C3) $\sigma_L < \sigma_0 < \sigma_U$ where σ_L and σ_U are known constants;
- (C4) $\|\eta_{0i}\| = O(1)$ for each $i = 1, \dots, n$;

Condition (C1) corresponds to the conditional likelihood of y_i given η_i being correctly specified, (C2) ensures that the covariance of the data does not grow too rapidly with p and the data contain increasing information on the latent factors as p increases—similar assumptions appear in the econometric factor model literature (Fan et al. 2008, 2011) and for massive covariance estimation problems (Pati et al. 2014). Condition (C3) states that the variance of the observed

y_i is bounded both above and below and (C4) is a weak assumption ensuring that the latent variables do not depend on n or p .

Lemma 1 gives sufficient conditions for the posterior probability on the space of partitions converging to the oracle probability for $p \rightarrow \infty$.

Lemma 1. *Let $\boldsymbol{\zeta}^{(p)} = (\zeta_1^{(p)}, \dots, \zeta_n^{(p)}) = \frac{1}{\sqrt{p}}(\Lambda^T \Lambda)^{1/2} \boldsymbol{\eta}$ and, for any $\delta > 0$,*

$$B_{p,\delta} = \bigcap_{i=1}^n \left\{ \Lambda, \eta_i : \frac{1}{\sqrt{p}} \|\Lambda \eta_i - \Lambda_0 \eta_{0i}\| < \delta \right\}.$$

Under (C1)-(C4), assume that for increasing p and for any $\delta > 0$

$$\Pi(\bar{B}_{p,\delta} \mid \mathbf{y}) \rightarrow 0 \quad \mathbb{P}_0^p\text{-a.s.} \quad (12)$$

where $\bar{B}_{p,\delta}$ is the complement of $B_{p,\delta}$. Let $E[\cdot \mid \mathbf{y}]$ denote expectations over the posterior distribution of the parameters given \mathbf{y} . Let $\Pi(\Psi \mid \boldsymbol{\zeta}^{(p)})$ be the posterior probability of partition Ψ with η_0 replaced by $\boldsymbol{\zeta}^{(p)}$ in (11). Then, $\lim_{p \rightarrow \infty} E \left[\Pi(\Psi \mid \boldsymbol{\zeta}^{(p)}) \mid \mathbf{y} \right] = \Pi(\Psi \mid \boldsymbol{\eta}_0)$.

The conditional probability $\Pi(\Psi \mid \boldsymbol{\zeta}^{(p)})$ depends on the Lamb model parameters. Lemma 1 shows that under condition (12), $\Pi(\Psi \mid \boldsymbol{\zeta}^{(p)})$ converges to the oracle partition probability in expectation. To show that Lamb satisfies condition (12) we consider an adaptation of Theorem 6.39 in Ghosal and Van Der Vaart (2017) in which, in place of having an increasing sample size, we assume an increasing data dimension with fixed sample size. This asymptotic notion is consistent with the idea that more and more variables are measured on each study subject. We introduce the following notation. Let $\vartheta = (\Lambda, \boldsymbol{\eta}, \sigma)$ with $\boldsymbol{\eta} = (\eta_1, \dots, \eta_n)$ and $\vartheta \in \Theta_p$. Let \mathbb{P}_ϑ^p and \mathbb{P}_0^p be the joint distributions of the data y_1, \dots, y_n given ϑ and ϑ_0 , respectively, with $\vartheta_0 = (\Lambda_0, \boldsymbol{\eta}_0, \sigma_0)$. We also denote the expectation of a function g with respect to \mathbb{P}_0^p and \mathbb{P}_ϑ^p by $\mathbb{P}_0^p g$ and $\mathbb{P}_\vartheta^p g$ respectively. Let p_0^p and p_ϑ^p be the densities of \mathbb{P}_0^p and \mathbb{P}_ϑ^p with respect to the Lebesgue measure. Finally, define the Kullback-Leibler (KL) divergence and the r -th order positive KL-variation between p_0^p and p_ϑ^p , respectively, as

$$KL(\mathbb{P}_0^p, \mathbb{P}_\vartheta^p) = \int \log \frac{p_0^p}{p_\vartheta^p} d\mathbb{P}_0^p; \quad V_r^+(\mathbb{P}_0^p, \mathbb{P}_\vartheta^p) = \int \left(\left(\log \frac{p_0^p}{p_\vartheta^p} - KL \right)^+ \right)^r d\mathbb{P}_0^p, \quad (13)$$

where f^+ denotes the positive part of a function f .

Theorem 2. *If for some $r \geq 2, c > 0$ there exist measurable sets $B_p \subset \Theta_p$ with $\liminf \Pi(B_p) > 0$,*

(I)

$$\sup_{\vartheta \in B_p} \frac{1}{p} KL(\mathbb{P}_0^p, \mathbb{P}_\vartheta^p) \leq c, \quad \sup_{\vartheta \in B_p} \frac{1}{p^r} V_r^+(\mathbb{P}_0^p, \mathbb{P}_\vartheta^p) \rightarrow 0, \quad (14)$$

(II) for sets $\tilde{\Theta}_p \subset \Theta_p$ there exists a sequence of test functions ϕ_p such that $\phi_p \rightarrow 0$ \mathbb{P}_0^p -a.s. and

$$\int_{\tilde{\Theta}_p} \mathbb{P}_\vartheta^p (1 - \phi_p) d\Pi(\vartheta) \leq e^{-Cp} \text{ for some } C > 0,$$

(III) letting $A_p = \left\{ \vartheta \in \Theta_p : \frac{1}{p} \int \left(\log \frac{p_\vartheta^p}{p_0^p} - KL(\mathbb{P}_0^p, \mathbb{P}_\vartheta^p) \right) d\tilde{\Pi}_p(\vartheta) < \tilde{\epsilon} \right\}$, with $\tilde{\Pi}_p$ the renormalized restriction of Π to set B_p , for any $\tilde{\epsilon} > 0$, $\mathbb{1}\{\bar{A}_p\} \rightarrow 0$ \mathbb{P}_0^p -a.s.,

then $\Pi(\tilde{\Theta}_p \mid \mathbf{y}) \rightarrow 0$ \mathbb{P}_0^p -a.s.

Condition (I) ensures that the assumed model is not too far from the true data-generating model. (II) controls the variability of the log-likelihood around its mean. In the Lamb model, the number of parameters grows with p and hence the assumption on V_r^+ is instrumental. The conditions on ϕ_p ensure the existence of a sequence of consistent test functions for $H_0 : \mathbb{P} = \mathbb{P}_0^p$ in which type-II error diminishes to 0 exponentially fast in the critical region. (III) is a technical condition required to bound the numerator of $\Pi(\tilde{\Theta}_p \mid \mathbf{y})$.

Theorem 2 is a general result stating sufficient conditions for posterior consistency as $p \rightarrow \infty$. The following Theorem, jointly with Lemma 1, shows that the case (i) Lamb model obtains the desired Bayesian oracle clustering property as $p \rightarrow \infty$.

Theorem 3. *For the case (i) Lamb model there exist a sequence of sets B_p such that conditions (I) and (III) are satisfied for any $c > 0$ and a sequence of test functions satisfying (II) with $\tilde{\Theta}_p = \bar{B}_{p,\delta}$ implying that $\Pi(\bar{B}_{p,\delta} \mid \mathbf{y}) \rightarrow 0$ \mathbb{P}_0^p -a.s.*

In Theorem 3 we are claiming that the conditions of Theorem 2 hold for the case (i) Lamb model. Its proof follows directly from Theorems 4- 5 proving (I), Theorem 6 proving (II), and Theorem 7 proving (III). All these theorems and the related proofs are reported in the Supplementary Materials.

5. PRACTICAL IMPLEMENTATION AND POSTERIOR COMPUTATION

5.1 Model specification

In this section, we develop a posterior computation algorithm for the case (iii) Lamb model; we focus on this case, since it is more flexible than cases (i)-(ii) and leads to better results

in simulations. In practice, the dimension d of the latent variables is unknown. Potentially we could put a prior on d , but this leads to substantially more expensive computation and hence we prefer an empirical Bayes approach that estimates d prior to running an MCMC algorithm. In particular, we perform an approximate sparse PCA decomposition of the data matrix and choose the smallest \hat{d} explaining at least 90% of the variability. We use the augmented implicitly restarted Lanczos bidiagonalization algorithm (Baglama and Reichel 2005) to obtain the approximate singular values and eigen vectors. The approximate eigen vectors are also used to initialize η in our MCMC implementation.

Although we consider a very broad class of Pitman-Yor mixtures in our theoretical results we simplify our computational implementation focusing on the Dirichlet-process mixture model in (5). As default choice we assume the DP precision parameter $\alpha = 1$. To complete a specification of our case (iii) Lamb model, we choose $(\mu_h, \Delta_h) \sim G_0$, with G_0 normal inverse-Wishart with location μ_0 , scale κ , inverse scale matrix Δ_0 and degrees of freedom ν . Following common practice, we choose μ_0 as a vector of zeros and $\Delta_0 = \delta I_d$ for some $\delta > 0$. For all our simulation experiments and practical application we have taken $\kappa_0 = 0.001$. Regarding δ , we consider two different default values. Although the Lamb model in its default form is for continuous data, we have also applied it to simulated discrete datasets mimicking the application in Section 7 where the original data are counts. Our default suggestion is to set $\delta = 20$. For situations involving data with ties, we chose lower values of δ . Our default choice is $\delta = 0.10$. Finally, for the Dirichlet-Laplace parameter, we set $a = 1$ and, following Bhattacharya and Dunson (2011), set $a_\sigma = 1$, $b_\sigma = 0.3$ in the prior on the residual error variances.

5.2 Posterior sampling

For posterior computation we propose the Gibbs sampler defined by the following steps.

Step 1 Sample the parameters related to the factor loadings Λ building on the algorithm of Bhattacharya et al. (2015). Specifically:

1. For $j = 1, \dots, p$ and $h = 1, \dots, d$ sample $\tilde{\psi}_{jh}$ independently from an inverse-Gaussian distribution $\text{iG}\left(\tau \frac{\phi_{jh}}{|\lambda_{jh}|}, 1\right)$ and set $\psi_{jh} = 1/\tilde{\psi}_{jh}$.
2. Sample the full conditional posterior distribution of τ from a generalized inverse Gaussian $\text{giG}\left(1 - dp, 1, 2 \sum_{j,h} \frac{|\lambda_{jh}|}{\phi_{jh}}\right)$ distribution.

3. To sample $\phi|\lambda$, draw T_{jh} independently with $T_{jh} \sim \text{giG}(a-1, 1, 2|\lambda_{jh}|)$ and set $\phi_{jh} = T_{jh}/T$ with $T = \sum_{jh} T_{jh}$.
4. Letting λ_j^T denote the j th row of Λ , for $j = 1, \dots, p$ sample

$$(\lambda_j | -) \sim \mathcal{N}_d \left((D_j^{-1} + \sigma_j^{-2} \eta^T \eta)^{-1} \eta^T \sigma_j^{-2} y^{(j)}, (D_j^{-1} + \sigma_j^{-2} \eta^T \eta)^{-1} \right),$$

where $\eta = (\eta_1, \dots, \eta_n)^T$, $D_j = \tau^2 \text{diag}(\psi_{j1} \phi_{j1}^2, \dots, \psi_{jd} \phi_{jd}^2)$ and $y^{(j)} = (y_{1j}, \dots, y_{nj})^T$.

Step 2 Update the cluster specific dispersion matrices Δ_h from the inverse-Wishart distribution $IW(\hat{\psi}_h, \hat{\nu}_h)$ where

$$\begin{aligned} \bar{\eta}_h &= \frac{1}{n_h} \sum_{i:c_i=h} \eta_i, \quad \hat{\nu}_h = \nu + n_h, \\ \hat{\psi}_h &= \delta^2 I_d + \sum_{i:c_i=h} (\eta_i - \bar{\eta}_h)(\eta_i - \bar{\eta}_h)^T + \frac{\kappa n_h}{\kappa + n_h} \bar{\eta}_h \bar{\eta}_h^T. \end{aligned}$$

Due to conjugacy the location parameter μ_h can be integrated out from the model.

Step 3 Sample the latent factors, for $i = 1, \dots, n$, from $(\eta_i | -) \sim \mathcal{N}_d(\Omega_h \rho_h, \Omega_h + \Omega_h(\hat{\kappa}_{h,-i} \Delta_h)^{-1} \Omega_h)$, where

$$\begin{aligned} n_{h,-i} &= \sum_{j \neq i} I_{c_j=h}, \quad \hat{\kappa}_{h,-i} = \kappa + n_{h,-i}, \\ \bar{\eta}_{h,-i} &= \frac{1}{n_{h,-i}} \sum_{j:c_j=h, j \neq i} \eta_j, \quad \hat{\mu}_{h,-i} = \frac{n_{h,-i} \bar{\eta}_{h,-i}}{n_{h,-i} + \kappa}, \\ \rho_h &= \Lambda^T \Sigma^{-1} Y_i + \Delta_h^{-1} \hat{\mu}_{h,-i}, \quad \Omega_h^{-1} = \Lambda^T \Sigma^{-1} \Lambda + \Delta_h^{-1}. \end{aligned}$$

Step 4 Following Algorithm 8 of Neal (2000), cluster indicator variables c_1, \dots, c_n can be sampled with probabilities

$$\begin{aligned} \Pi(c_i = h | -) &\propto n_{h,-i} \int \mathcal{N}_d(\eta_i; \mu_h, \Delta_h) d\Pi(\mu_h, \Delta_h | \eta_{-i}) \quad \text{for } h \in \{c_j\}_{j \neq i}, \\ \Pi(c_i \neq c_j \text{ for all } j \neq i | -) &\propto \alpha \int \mathcal{N}_d(\eta_i; \mu_h, \Delta_h) d\Pi(\mu_h, \Delta_h), \end{aligned} \tag{15}$$

where η_{-i} is the set of all η_j , $j = 1, \dots, n$ except η_i . Due to conjugacy the closed form

of the integrals in (15) are analytically available and

$$\int \mathcal{N}_d(\eta_i; \mu_h, \Delta_h) d\Pi(\mu_h, \Delta_h \mid \eta_{-i}) = t_{\hat{\nu}_{h,-i}-d+1} \left(\eta_i; \hat{\mu}_{h,-i}, \hat{\psi}_{h,-i} \right)$$

where

$$\begin{aligned} \hat{\nu}_{h,-i} &= \nu + n_{h,-i}, \\ \hat{\psi}_{h,-i} &= \frac{\hat{\kappa}_{h,-i} + 1}{\hat{\kappa}_{h,-i}(\hat{\nu}_{h,-i} - d + 1)} \times \\ &\quad \left[\delta^2 I_d + \sum_{j: c_j = h, j \neq i} (\eta_j - \bar{\eta}_{h,-i})(\eta_j - \bar{\eta}_{h,-i})^T + \frac{\kappa n_{h,-i}}{\kappa + n_{h,-i}} \bar{\eta}_{h,-i} \bar{\eta}_{h,-i}^T \right] \end{aligned}$$

and $t_\nu(\cdot; \mu, \Delta)$ is the multivariate central t -distribution with degrees of freedom ν , location μ and scale matrix Δ .

Step 5 For $j = 1, \dots, p$ sample σ_j^2 independently from

$$(\sigma_j^{-2} \mid -) \sim \text{Ga} \left(a_\sigma + \frac{n}{2}, b_\sigma + \frac{1}{2} \sum_{i=1}^n (y_{ij} - \lambda_j^T \eta_i)^2 \right).$$

Despite its simplicity, the Gibbs sampler can sometimes get stuck in local modes (Gilks et al. 1996, Chapter 6). In particular, a key bottleneck is the exploration Step 4. Therefore, we adopt the split-merge MCMC procedure proposed by Jain and Neal (2004). Dunson and Johndrow (2019) discuss that split-merge procedures can offer dramatic improvements over Gibbs sampling especially in high dimensions. Jain and Neal (2004) note that the Gibbs sampler is useful in moving singleton samples between clusters while the split-merge algorithm addresses the problem of making major changes. To gain both benefits, we randomly switch between Gibbs and split-merge updates of the cluster indicator variables. The split-merge algorithm makes smart proposals by performing restricted Gibbs scans which are of exactly same form as in (15).

6. SIMULATION STUDY

We performed a simulation study to analyze the performance of Lamb in clustering high dimensional data. The Gibbs sampler introduced in Section 5.2 has been implemented in **C++** and ported to R using the **Rcpp** package (Eddelbuettel and François 2011). Code can be obtained from the first author GitHub page. Lamb is compared with different competitors: a Dirichlet

process mixture of Gaussian (DPM) model with diagonal covariance matrix as implemented in the R package `BNPmix` (Corradin et al. 2019), a nonparametric mixture of (infinite) factor analyzers (MFA) as implemented in the R package `IMIFA` (Murphy et al. 2019), and a pragmatical two-step approach (PCA-KM) that performs an approximate sparse principal component analysis of the high dimensional data to reduce the dimensionality from p to d —with d being the minimum number of components explaining at least the 90% of the total variability consistently with the discussion of Section 5—and then applies a k-means algorithm on the first principal components, with k chosen using the silhouettes method (Rousseeuw 1987). For the high-dimensional simulation settings we considered, DPM and MFA showed high instability (lack of convergence, memory errors, extremely long running time, etc). For these reasons we report a comparison with the PCA-KM approach only.

We generated data under three different mixture model scenarios, with there being a true cluster membership in each case. The main goal is to test the accuracy of the estimated clustering relative to the true clustering. To this end, we compute the adjusted Rand index (Rand 1971) as implemented in the `mclust` package (Scrucca et al. 2016).

For each scenario, we vary the true number of clusters $k_0 \in \{7, 15, 30\}$, with 2/3 of the clusters having the same probability of being observed and the remaining 1/3 of the clusters having together the same probability of a single “main” cluster. For example if $k_0 = 15$, we set 10 main clusters with probability 0.09 each and 5 minor clusters of equal weight whose total probability sums to 0.09. This is a challenging scenario as many methods struggle outside of the setting in which there is a small number of common clusters that are well separated, even in small to moderate dimensional settings. We consider: mixture of factor analyzers (Scenario 1), type (iii) Lamb (Scenario 2), and mixture of log transformed zero inflated Poisson (Scenario 3). The first two scenarios have a latent structure of dimension 35, while Scenario 3 is particularly challenging as the data are discrete and the cluster-specific distributions are highly non-Gaussian; this is done to assess robustness and mimic the scRNASeq data structure analyzed in Section 7. The dimension p varies in $p = \{2500, 5000\}$ while the sample size n is fixed to $n = 2000$.

We compute posterior clustering summaries for Lamb following Wade and Ghahramani (2018) and using their R implementation. Our point estimate is the partition visited by the MCMC sampler that minimizes the posterior expectation of the Binder loss exploiting the posterior similarity matrix obtained from the different sampled partitions.

We run our sampler for 11000 iterations discarding the first 2000 as burn in and taking one draw every five to reduce autocorrelation. Prior elicitation follows the default specification discussed in Section 5. On average a single run under these settings took between 40 and 50 minutes on a iMac with 4.2 GHz Quad-Core Intel Core i7 processor and 32GB DDR4 RAM.

The results are reported in Table 1. Both approaches perform reasonably well in Scenarios 1 and 3 with PCA-KM showing poor performance in Scenario 2. However, Lamb is uniformly superior in each scenario obtaining very high adjusted Rand indices suggesting accurate estimation of the clustering structure in the data. An appealing aspect of taking a Bayesian approach is that uncertainty in clustering is characterized through the posterior distribution; Wade and Ghahramani (2018) discuss various ways to present this uncertainty in practice. We report in Table 1 95% posterior credible intervals for the adjusted Rand index, computed taking the empirical quantiles of the adjusted Rand indices calculated for each visited partition. These intervals are very narrow suggesting negligible posterior variability around the point estimates. Visual inspection of the traceplots of each observation’s cluster membership, indeed, confirms this with only a small portion of observations moving from one partition to another during the Gibbs sampler after burn-in. Based on the results, Lamb rarely overestimates the true number of clusters. This suggests that the small estimation errors are mainly due to the merging of similar clusters, showing a propensity towards more parsimonious clustering structures. This is particularly evident for the simulations with $k_0 = \{15, 30\}$ in Scenarios 1–2, where many of the smallest clusters (each contributing with $\approx 0.5\%$ of the observations) are merged. In simulating the data, we did not restrict clusters to be well separated and clusters could be very close to each other so such merging is appealing. The UMAP (McInnes et al. 2018) projections of the data reported in the Supplementary Materials give a visual representation of this.

It is important to consider the impact of the hyperparameter choice on the results. Instead of conducting a detailed sensitivity analysis by rerunning the algorithms for each simulated dataset and for many different choices of hyperparameter values, we took the approach of carefully choosing default choices of hyperparameters that we then used in each of the simulated and real data cases. We have found our recommended hyperparameter values to yield good performance in each of the cases we have considered. We also did a small sensitivity analysis based on perturbing key hyperparameters, and found the results to be robust in general. However, there can be sensitivity to δ , the scale of the Normal inverse-Wishart base measure, particularly when data have ties as in Scenario 3. In this case, if we set δ close to zero, the algorithm can produce

Table 1: Simulation results for PCA-KM and Lamb methods. Adjusted Rand index (and 95% credible intervals for Lamb) and estimated number of clusters.

		k_0	adjusted Rand index			# of clusters	
			PCA-KM	Lamb	(95% CI)	PCA-KM	Lamb
Scenario 1	$p = 2500$	7	1.000	1.000	(0.999, 1.000)	7	7
		15	0.898	0.991	(0.991, 0.991)	13	13
		30	0.867	0.996	(0.991, 0.997)	21	25
	$p = 5000$	7	1.000	0.945	(0.945, 1.000)	7	6
		15	0.879	0.999	(0.987, 0.999)	13	16
		30	0.922	0.996	(0.990, 0.998)	28	30
Scenario 2	$p = 2500$	7	0.257	1.000	(1.000, 1.000)	2	7
		15	0.165	0.949	(0.948, 0.981)	2	11
		30	0.089	0.966	(0.965, 0.966)	2	21
	$p = 5000$	7	0.305	1.000	(1.000, 1.000)	2	7
		15	0.168	0.961	(0.960, 0.961)	2	11
		30	0.000	0.969	(0.969, 0.969)	2	21
Scenario 3	$p = 2500$	7	0.834	0.948	(0.947, 0.948)	9	6
		15	0.779	0.986	(0.985, 0.986)	24	17
		30	0.786	0.974	(0.974, 0.974)	38	30
	$p = 5000$	7	0.901	0.948	(0.948, 0.948)	7	6
		15	0.787	0.986	(0.985, 0.986)	23	17
		30	0.759	0.976	(0.976, 0.976)	47	28

too many clusters—this may be due to the model misspecification favoring splitting of a single cluster into several to better explain the zero inflated log-Poisson shape and/or the ties.

7. CELL LINE DATA APPLICATION

In this section, the GSE81861 cell line dataset (Li et al. 2017) is used as a test for the proposed clustering method. The dataset is obtained profiling 630 single cells from 7 cell lines using the Fluidigm based single cell RNA-seq protocol (See et al. 2018). The dataset includes 83 A549 cells, 65 H1437 cells, 55 HCT116 cells, 23 IMR90 cells, 96 K562 cells, and 134 GM12878 cells (38 from batch 1, 96 from batch 2), 174 H1 cells (96 from batch 1, 78 from batch 2) and 57,241 genes. In this dataset, the cell-types are known and hence the data provide a useful benchmark to assess the performance of our novel model-based clustering procedure.

Following standard practice in single cell data analysis, we start by applying data pre-processing steps (Andrews and Hemberg 2018a). Cells with low read counts are discarded, as we lack reliable gene expression measurements for these cells. Multiplexed-sequencing of scRNASeq

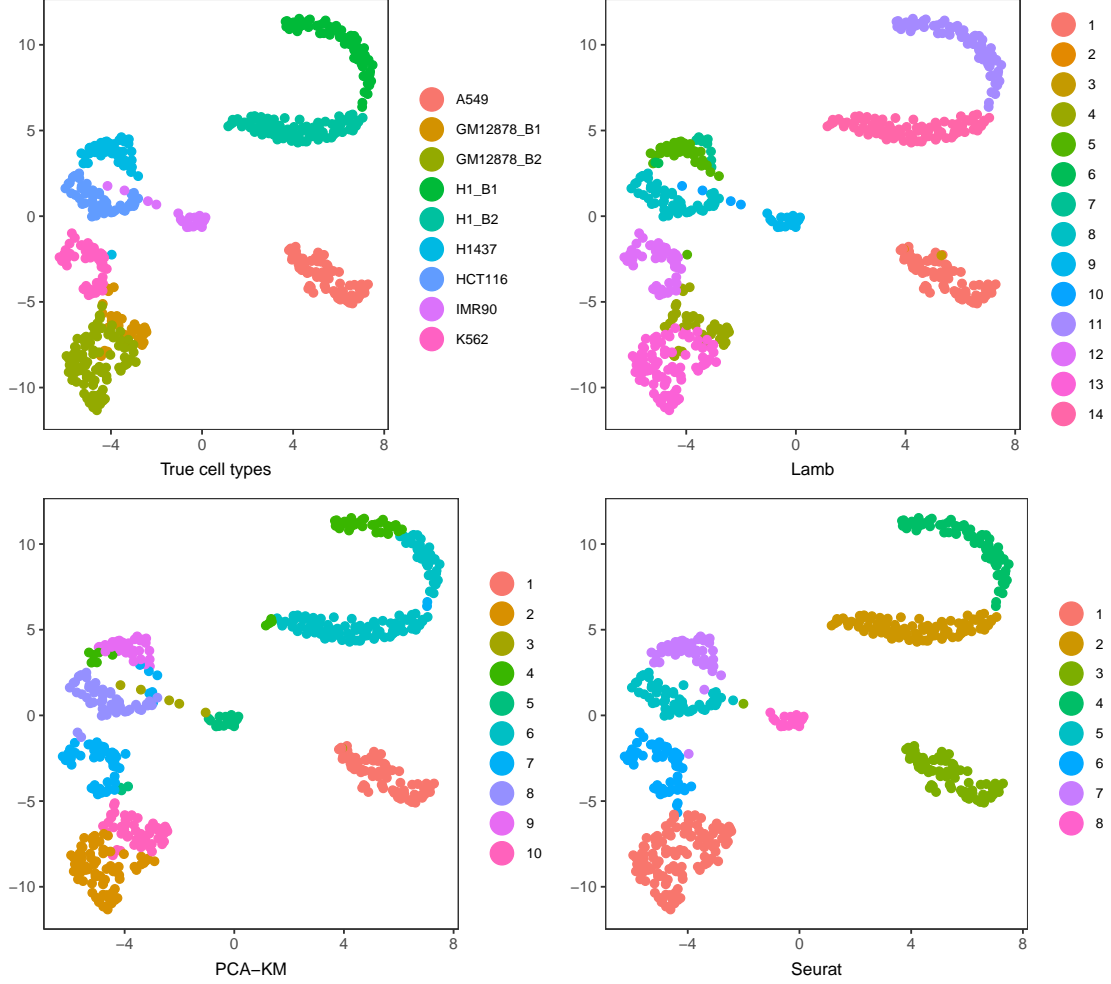


Figure 1: UMAP plots of the cell line dataset: different panels use different color legends: (a) true clustering; (b) Lamb estimate; (c) PCA-KM estimate; (d) Seurat estimate

results in unequal numbers of reads across cells and a normalization procedure is typically implemented before downstream analysis. For this dataset, this step has been performed using the SCRAN normalization technique (Lun et al. 2016). After normalization data have been \log_2 transformed and then scaled to have unit variance and zero mean. Before running our clustering methods, we remove uninformative genes in order to reduce both the noise and the computational burden without losing too much information. Specifically we remove the non-informative genes using the M3Drop tool (Andrews and Hemberg 2018b), as commonly done in this context. After this pre-processing phase, we obtain a final dataset with $n = 531$ cells and $p = 14,804$ genes.

An appealing aspect of our approach is it provides coherent Bayesian posterior uncertainty quantification. The 99% credible interval for the adjusted Rand index is $[0.939, 0.960]$ and the posterior probability of having 14 clusters is 0.726 with a 99% credible interval of $[13, 15]$. This suggests that the posterior distribution is highly concentrated, which is consistent with our simulations. The posterior similarity matrix reported in the first panel of Figure 2—also reporting the related dendrogram obtained by using complete linkage—clearly shows that the majority of the observations have a high posterior probability of being assigned to a specific cluster and negligible probability of being assigned to an incorrect cluster. Figure 2 also points out the presence of the micro clusters that caused the overestimation of Λ for this specific dataset. To better examine this outcome, in the right panel of the same figure, we zoom in on the upper right corner of the similarity matrix. Two cells of cluster A549 are put in singleton clusters. Their probability of being merged in a single cluster is 0.22 but the posterior probability of being merged to their main cluster is negligible. Similarly cluster IMR90 is divided into two clusters with one of them (cluster 10, according to our labelling) being very small. Finally cluster H1437 is split into two clusters (clusters 5 and 6 according to our labelling) with the smallest one comprising just two observations. Introduction of such micro-clusters has minimal impact on the adjusted Rand index, which is clearly much higher for Λ than the competitors, and is a minor practical issue that is not unexpected given the tendency of Dirichlet process mixture models to favor some tiny or even singleton clusters. These clusters may even be ‘real’ given that the cell type labels are not a perfect gold standard.

8. DISCUSSION

Part of the appeal of Bayesian methods comes through the intrinsic penalty for model complexity or ‘Bayesian Ockham razor’ (Jefferys and Berger 1992). This penalty comes in through integrating the likelihood over the prior in obtaining the marginal likelihood; if one inappropriately adds extra unnecessary parameters to the model, then this leads to integrating the likelihood over a larger region, which tends to reduce the marginal likelihood. In clustering problems, one relies on the Bayesian Ockham razor to choose the appropriate compromise between the two extremes of too many clusters and over-fitting and too few clusters and under-fitting. Often in low-dimensional problems, the Bayesian Ockham razor is effective and one obtains a posterior providing a reasonable representation of uncertainty in clustering data into groups of relatively similar observations. However, a key contribution of this article is showing that this is fun-

damentally not the case in high-dimensional problems, and one can often obtain nonsensical results using seemingly reasonable priors.

Perhaps the most interesting aspect of our paper is the negative result showing degenerate behavior in the $p \rightarrow \infty$ case for the true posterior on clusterings, regardless of the true data generating model. This negative result provided motivation for our simple Lamb model, which reduces the large p pitfall by clustering on the latent variable level. Another interesting theoretical result is our notion of a Bayesian oracle for clustering; to our knowledge, there is not a similar concept in the literature. We hope that this new oracle can be used in evaluating other Bayesian procedures for high-dimensional clustering, providing competitors to the simple Lamb model.

We view the proposed model as a simple first step towards addressing pitfalls of Bayesian approaches to high-dimensional clustering. There are several important aspects that we have not been able to address in this initial paper. The first is the issue of fast computation in very large p clustering problems. We have taken a relatively simple MCMC approach that works adequately well in our motivating application in which one has the luxury of running the analysis for many hours for each new dataset. However, there is certainly a need for much faster algorithms that can exploit parallel and distributed processing; for example, running MCMC for different subsets of the variables in parallel and combining the results. Potentially building on the algorithms of Wang and Dunson (2013) and Scott et al. (2016) may be promising in this regard.

Another critical issue in Bayesian and other model-based clustering is the issue of model misspecification. In particular, clusters may not have Gaussian shapes or may not even match with more elaborate kernels, such as skewed Gaussians (Azzalini 2013). There is an evolving literature for addressing this problem in low dimensions using mixtures of mixtures (Miller and Harrison 2018) and generalized Bayes methods (e.g. Miller and Dunson 2019) however, it is not clear that current methods of this type can scale up to the types of dimensions encountered in our motivating genomic applications. One possibility is to rely on variational Bayes methods, such as variational autoencoders (Kingma et al. 2014; Rezende et al. 2014); however, then one faces challenging issues in terms of obtaining reliable algorithms having theoretical guarantees, generalizability and reproducibility.

ACKNOWLEDGMENTS

This work was partially funded by grants R01-ES027498 and R01-ES028804 from the National Institute of Environmental Health Sciences of the United States Institutes of National Health and by the University of Padova under the STARS Grant.

APPENDIX

Proofs of Section 2

Proof of Theorem 1. Consider the ratio of posterior probabilities:

$$\frac{\Pi\{\Psi \mid \mathbf{y}\}}{\Pi\{\Psi' \mid \mathbf{y}\}}. \quad (\text{A.1})$$

If this ratio converges to zero for all c_1, \dots, c_n in f_0 -probability as $p \rightarrow \infty$, then any partition nested into another partition is more likely *a posteriori* implying $\Pi(c_1 = \dots = c_n \mid \mathbf{y}) = 1$ so that all subjects are grouped in the same cluster with probability one. Conversely if the ratio converges to $+\infty$, then $\Pi(c_1 \neq \dots \neq c_n \mid \mathbf{y}) = 1$ and each subject is assigned to their own cluster with probability one.

Without loss of generality, assume that c_1, \dots, c_n define k clusters of sizes n_1, \dots, n_k and that $c'_i = c_i$ for $c_i \in \{1, \dots, k-2\}$ and $c'_i = k-1$ for $c_i \in \{k-1, k\}$, with n'_1, \dots, n'_k the cluster sizes under the partition induced by the c'_i . In general, ratio (A.1) can be expressed as

$$\frac{\Pi(\Psi)}{\Pi(\Psi')} \times \frac{\prod_{h=1}^k \int \prod_{i:c_i=h} \mathcal{K}(y_i; \theta) dP_0(\theta)}{\prod_{h=1}^{k-1} \int \prod_{i:c'_i=h} \mathcal{K}(y_i; \theta) dP_0(\theta)}. \quad (\text{A.2})$$

The left hand site of (A.2) can be expressed as the ratio between the EPPFs. For the Pitman-Yor process, the numerator is

$$\frac{\prod_{j=1}^k \Gamma(n_j + 1)}{\Gamma(n + 1)} \frac{\prod_{j=1}^{k-1} (\alpha + j\sigma)}{(\alpha + 1)_{n-1}} \prod_{j=1}^k (1 - \sigma)_{n_j - 1}$$

which, in the DP case becomes

$$\frac{\prod_{j=1}^k \Gamma(n_j + 1)}{\Gamma(n + 1)} \frac{\alpha^k}{(\alpha)_n} \prod_{j=1}^k \Gamma(n_j),$$

where $(a)_n = a(a+1) \dots (a+n-1)$ is the rising factorial operator. Hence, the left hand side

of (A.2) simplifies to

$$\frac{\Gamma(n_{k-1}+1)\Gamma(n_k+1)}{\Gamma(n_{k-1}+n_k+1)} (\alpha + (k-1)\sigma) \frac{(1-\sigma)_{n_{k-1}-1}(1-\sigma)_{n_k-1}}{(1-\sigma)_{n_{k-1}+n_k-1}}, \text{ and}$$

$$\frac{\Gamma(n_{k-1}+1)\Gamma(n_k+1)}{\Gamma(n_{k-1}+n_k+1)} \alpha,$$

for the Pitman–Yor and the Dirichlet processes, respectively, and hence are constants for $p \rightarrow \infty$ and independent from f_0 . Thus, by induction and under the assumptions on the right factor of (A.2) we conclude the proof. \square

Proof of Corollary 1. Let c_1, \dots, c_n and c'_1, \dots, c'_n consistently with the proof of Theorem 1. Then, consider the ratio of the marginal likelihoods

$$\frac{\int \prod_{h=1}^k \int \prod_{i:c_i=h} \mathcal{N}_p(y_i; \mu_h \mathbf{1}_p, \sigma^2 I_p) \mathcal{N}(\mu_h; \mu_0, \kappa_0^{-1} \sigma^2) IG(\sigma^2; \nu_0, \lambda_0) d\mu_h d\sigma^2}{\int \prod_{h=1}^{k-1} \int \prod_{i:c'_i=h} \mathcal{N}_p(y_i; \mu_h \mathbf{1}_p, \sigma^2 I_p) \mathcal{N}(\mu_h; \mu_0, \kappa_0^{-1} \sigma^2) IG(\sigma^2; \nu_0, \lambda_0) d\mu_h d\sigma^2}. \quad (\text{A.3})$$

The numerator of (A.3) is

$$(2\pi)^{n/2} \frac{\Gamma(\nu_0 + np/2)}{\Gamma(\nu_0)} \prod_{h=1}^k \left(\frac{\kappa_0}{n_h p + \kappa_0} \right)^{\frac{1}{2}} \times \left[\lambda_0 / \left(\lambda_0 + \sum_{h=1}^k \left\{ S_h^\Psi + \frac{\kappa_0 n_h p}{n_h p + \kappa_0} (\bar{y}_h^\Psi - \mu_0)^2 \right\} \right) \right]^{\nu_0 + \frac{np}{2}},$$

with $\bar{y}_h^\Psi = \frac{1}{n_h p} \sum_{i:c_i=h} \sum_{j=1}^p y_{ij}$, and $S_h^\Psi = \sum_{i:c_i=h} \sum_{j=1}^p (y_{ij} - \bar{y}_h^\Psi)^2$. Obtaining a corresponding expression for the denominator, the ratio (A.3) becomes

$$\left(\frac{\kappa_0(\kappa_0 + n'_{k-1}p)}{(\kappa_0 + n_k p)(\kappa_0 + n_{k-1}p)} \right)^{\frac{1}{2}} \left[\frac{\lambda_0 + \sum_{h=1}^{k-1} \left\{ S_h^{\Psi'} + \frac{\kappa_0 n'_h p}{n'_h p + \kappa_0} (\bar{y}_h^{\Psi'} - \mu_0)^2 \right\}}{\lambda_0 + \sum_{h=1}^k \left\{ S_h^\Psi + \frac{\kappa_0 n_h p}{n_h p + \kappa_0} (\bar{y}_h^\Psi - \mu_0)^2 \right\}} \right]^{\nu_0 + \frac{np}{2}}. \quad (\text{A.4})$$

If we replace each observation y_i with $\tilde{y}_i = y_i - \mu_0 \mathbf{1}_p$, the assumption on y_i is still valid for \tilde{y}_i . Hence, without loss of generality we can assume $\mu_0 = 0$. We need to show the denominator of the term in $[\cdot]$ is smaller than the numerator. Due to the structure of the partitions, the first

$k - 2$ terms in the relevant summations are equal, as for $h < k - 1$, we have

$$S_h^\Psi + \frac{\kappa_0 n_h p}{n_h p + \kappa_0} (\bar{y}_h^\Psi)^2 = S_h^{\Psi'} + \frac{\kappa_0 n'_h p}{n'_h p + \kappa_0} (\bar{y}_h^{\Psi'})^2.$$

Hence, we can focus on the difference between the $k - 1$ term in the numerator and the $k + (k - 1)$ terms in the denominator. Note that

$$\begin{aligned} & \frac{1}{p} \left[S_{k-1}^{\Psi'} - S_k^\Psi - S_{k-1}^\Psi + \frac{\kappa_0 (n_{k-1} + n_k) p}{(n_{k-1} + n_k) p + \kappa_0} (\bar{y}_{k-1}^{\Psi'})^2 - \sum_{h=k-1}^k \frac{\kappa_0 n_h p}{n_h p + \kappa_0} (\bar{y}_h^\Psi)^2 \right] \\ &= \left[\sum_{h=k-1}^k n_h (\bar{y}_h^\Psi)^2 - (n_{k-1} + n_k) (\bar{y}_{k-1}^{\Psi'})^2 \right] \\ & \quad + \frac{1}{p} \left[\frac{\kappa_0 (n_{k-1} + n_k) p}{(n_{k-1} + n_k) p + \kappa_0} (\bar{y}_{k-1}^{\Psi'})^2 - \sum_{h=k-1}^k \frac{\kappa_0 n_h p}{n_h p + \kappa_0} (\bar{y}_h^\Psi)^2 \right]. \end{aligned} \quad (\text{A.5})$$

By Jensen's inequality the term inside the first parenthesis is strictly positive. In addition, since $p \left(\frac{1}{p} \sum_j y_{ij} \right)^2 \leq \|y_i\|^2 = O_p(p)$ for all i , the second additive term of (A.5) goes to 0 as $p \rightarrow \infty$ and therefore for large enough p ,

$$\frac{1}{p} \left[\lambda_0 + \sum_{h=1}^{k-1} \left\{ S_h^{\Psi'} + \frac{\kappa_0 n'_h p}{n'_h p + \kappa_0} (\bar{y}_h^{\Psi'})^2 \right\} \right] > \frac{1}{p} \left[\lambda_0 + \sum_{h=1}^k \left\{ S_h^\Psi + \frac{\kappa_0 n_h p}{n_h p + \kappa_0} (\bar{y}_h^\Psi)^2 \right\} \right]. \quad (\text{A.6})$$

Now taking the \liminf of $\frac{1}{p} \log$ (A.4) we have

$$\begin{aligned} & \liminf_{p \rightarrow \infty} \left[\frac{1}{p} \log \left(\frac{\kappa_0 (\kappa_0 + n'_{k-1} p)}{(\kappa_0 + n_k p)(\kappa_0 + n_{k-1} p)} \right)^{\frac{1}{2}} \right. \\ & \quad \left. + \frac{1}{p} \log \left[\frac{\lambda_0 + \sum_{h=1}^{k-1} \left\{ S_h^{\Psi'} + \frac{\kappa_0 n'_h p}{n'_h p + \kappa_0} (\bar{y}_h^{\Psi'})^2 \right\}}{\lambda_0 + \sum_{h=1}^k \left\{ S_h^\Psi + \frac{\kappa_0 n_h p}{n_h p + \kappa_0} (\bar{y}_h^\Psi)^2 \right\}} \right]^{\nu_0 + \frac{n p}{2}} \right] \\ &= \frac{n}{2} \liminf_{p \rightarrow \infty} \log \left[\frac{\frac{1}{p} \left\{ \lambda_0 + \sum_{h=1}^{k-1} \left\{ S_h^{\Psi'} + \frac{\kappa_0 n'_h p}{n'_h p + \kappa_0} (\bar{y}_h^{\Psi'})^2 \right\} \right\}}{\frac{1}{p} \left\{ \lambda_0 + \sum_{h=1}^k \left\{ S_h^\Psi + \frac{\kappa_0 n_h p}{n_h p + \kappa_0} (\bar{y}_h^\Psi)^2 \right\} \right\}} \right] > 0 \text{ from (A.6),} \end{aligned}$$

which concludes the proof. \square

Proof of Corollary 2. The proof follows along the lines of the proof of Corollary 1. Let c_1, \dots, c_n

and c'_1, \dots, c'_n consistently with the proof of Theorem 1. Then, consider the ratio of the marginal likelihoods

$$\frac{\int \prod_{h=1}^k \int \prod_{i:c_i=h} \mathcal{N}_p(y_i; \mu_h, \Sigma) \mathcal{N}_p(\mu_h; \mu_0, \kappa_0^{-1}\Sigma) d\mu_h IW(\Sigma; \nu_0, \Lambda_0) d\Sigma}{\int \prod_{h=1}^{k-1} \int \prod_{i:c'_i=h} \mathcal{N}_p(y_i; \mu_h, \Sigma) \mathcal{N}_p(\mu_h; \mu_0, \kappa_0^{-1}\Sigma) d\mu_h IW(\Sigma; \nu_0, \Lambda_0) d\Sigma}. \quad (\text{A.7})$$

Its numerator is

$$\begin{aligned} & \int \prod_{h=1}^k \int \prod_{i:c_i=h} \mathcal{N}_p(y_i; \mu_h, \Sigma) \mathcal{N}_p(\mu_h; \mu_0, \kappa_0^{-1}\Sigma) d\mu_h IW(\Sigma; \nu_0, \Lambda_0) d\Sigma \\ &= (\pi)^{-\frac{np}{2}} \frac{\Gamma_p(\frac{\nu_0+n}{2})}{\Gamma_p(\nu_0/2)} |\Lambda_0|^{\nu_0/2} \prod_{h=1}^k \left(\frac{\kappa_0}{n_h + \kappa_0} \right)^{\frac{p}{2}} \times \\ & \quad \left| \Lambda_0 + \sum_{h=1}^k \left\{ S_h^\Psi + \frac{n_h \kappa_0}{n_h + \kappa_0} (\bar{y}_h^\Psi - \mu_0)(\bar{y}_h^\Psi - \mu_0)^T \right\} \right|^{-\frac{\nu_0+n}{2}} \end{aligned}$$

where

$$\bar{y}_h^\Psi = \frac{1}{n_h} \sum_{i:c_i=h} y_i, \quad S_h^\Psi = \sum_{i:c_i=h} (y_i - \bar{y}_h^\Psi)(y_i - \bar{y}_h^\Psi)^T.$$

Hence, obtaining a corresponding expression for the denominator, ratio A.7 becomes

$$\left(\frac{\kappa_0(\kappa_0 + n'_{k-1})}{(\kappa_0 + n_{k-1})(\kappa_0 + n_k)} \right)^{p/2} \left(\frac{\left| \Lambda_0 + \sum_{h=1}^{k-1} \left\{ S_h^{\Psi'} + \frac{n'_h \kappa_0}{n'_h + \kappa_0} (\bar{y}_h^{\Psi'} - \mu_0)(\bar{y}_h^{\Psi'} - \mu_0)^T \right\} \right|}{\left| \Lambda_0 + \sum_{h=1}^k \left\{ S_h^\Psi + \frac{n_h \kappa_0}{n_h + \kappa_0} (\bar{y}_h^\Psi - \mu_0)(\bar{y}_h^\Psi - \mu_0)^T \right\} \right|} \right)^{\frac{\nu_0+n}{2}}.$$

First note that for $n_k, n_{k-1} \geq 1$

$$\frac{\kappa_0(\kappa_0 + n'_{k-1})}{(\kappa_0 + n_{k-1})(\kappa_0 + n_k)} < 1. \quad (\text{A.8})$$

Similar to Corollary 1, we can assume without loss of generality μ_0 to be a p -dimensional vector of zero as if we replace each observation y_i with $\tilde{y}_i = y_i - \mu_0$ the assumption on y_i is still valid for \tilde{y}_i . Similarly the structure of the partitions Ψ and Ψ' is such that

$$S_h^\Psi + \frac{n_h \kappa_0}{n_h + \kappa_0} \bar{y}_h^\Psi \bar{y}_h^{\Psi T} = S_h^{\Psi'} + \frac{n'_h \kappa_0}{n'_h + \kappa_0} \bar{y}_h^{\Psi'} \bar{y}_h^{\Psi' T},$$

for all $h < k - 1$. Hence,

$$\begin{aligned} & \sum_{h=1}^k \left[S_h^\Psi + \frac{n_h \kappa_0}{n_h + \kappa_0} \bar{y}_h^\Psi \bar{y}_h^{\Psi T} \right] - \sum_{h=1}^{k-1} \left[S_h^{\Psi'} + \frac{n'_h \kappa_0}{n'_h + \kappa_0} \bar{y}_h^{\Psi'} \bar{y}_h^{\Psi' T} \right] \\ &= S_k^\Psi + S_{k-1}^\Psi - S_{k-1}^{\Psi'} - \kappa_0 \left[\frac{n'_{k-1}}{n'_{k-1} + \kappa_0} \bar{y}_{k-1}^{\Psi'} \bar{y}_{k-1}^{\Psi' T} - \sum_{h=k-1}^k \frac{n_h}{n_h + \kappa_0} \bar{y}_h^\Psi \bar{y}_h^{\Psi T} \right]. \end{aligned}$$

With the convention that the notation $A \preceq B$, with A and B square matrices, means that $B - A$ is positive definite, we can note that

$$n'_{k-1} \bar{y}_{k-1}^{\Psi'} \bar{y}_{k-1}^{\Psi' T} \preceq n_{k-1} \bar{y}_{k-1}^\Psi \bar{y}_{k-1}^{\Psi T} + n_k \bar{y}_k^\Psi \bar{y}_k^{\Psi T}$$

and hence also

$$\frac{n'_{k-1}}{n'_{k-1} + \kappa_0} \bar{y}_{k-1}^{\Psi'} \bar{y}_{k-1}^{\Psi' T} \preceq \frac{n_{k-1}}{n_{k-1} + \kappa_0} \bar{y}_{k-1}^\Psi \bar{y}_{k-1}^{\Psi T} + \frac{n_k}{n_k + \kappa_0} \bar{y}_k^\Psi \bar{y}_k^{\Psi T}.$$

Also $S_{k-1}^{\Psi'} \preceq S_k^\Psi + S_{k-1}^\Psi$ and thus

$$S_{k-1}^{\Psi'} + \frac{n'_{k-1} \kappa_0}{n'_{k-1} + \kappa_0} \bar{y}_{k-1}^{\Psi'} \bar{y}_{k-1}^{\Psi' T} \preceq \left\{ S_k^\Psi + \frac{n_k \kappa_0}{n_k + \kappa_0} \bar{y}_k^\Psi \bar{y}_k^{\Psi T} \right\} + \left\{ S_{k-1}^\Psi + \frac{n_{k-1} \kappa_0}{n_{k-1} + \kappa_0} \bar{y}_{k-1}^\Psi \bar{y}_{k-1}^{\Psi T} \right\}.$$

Hence considering the related determinants we have

$$\left| \Lambda_0 + \sum_{h=1}^{k-1} \left\{ S_h^{\Psi'} + \frac{n'_h \kappa_0}{n'_h + \kappa_0} \bar{y}_h^{\Psi'} \bar{y}_h^{\Psi' T} \right\} \right| < \left| \Lambda_0 + \sum_{h=1}^k \left\{ S_h^\Psi + \frac{n_h \kappa_0}{n_h + \kappa_0} \bar{y}_h^\Psi \bar{y}_h^{\Psi T} \right\} \right|. \quad (\text{A.9})$$

Therefore taking $\frac{1}{p} \log$ of (A.7)

$$\frac{1}{2} \log \frac{\kappa_0 (\kappa_0 + n'_{k-1})}{(\kappa_0 + n_{k-1})(\kappa_0 + n_k)} - \frac{n + \nu_0}{2p} \log \frac{\left| \Lambda_0 + \sum_{h=1}^k \left\{ S_h^\Psi + \frac{n_h \kappa_0}{n_h + \kappa_0} \bar{y}_h^\Psi \bar{y}_h^{\Psi T} \right\} \right|}{\left| \Lambda_0 + \sum_{h=1}^{k-1} \left\{ S_h^{\Psi'} + \frac{n'_h \kappa_0}{n'_h + \kappa_0} \bar{y}_h^{\Psi'} \bar{y}_h^{\Psi' T} \right\} \right|}.$$

From (A.8), (A.9) and by the assumption on ν_0 we can conclude that

$$\limsup_{p \rightarrow \infty} \frac{1}{p} \log \frac{\int \prod_{h=1}^k \int \prod_{i:c_i=h} \mathcal{N}_p(y_i; \mu_h, \Sigma) \mathcal{N}_p(\mu_h; \mu_0, \kappa_0^{-1} \Sigma) d\mu_h IW(\Sigma; \nu_0, \Lambda_0) d\Sigma}{\int \prod_{h=1}^{k-1} \int \prod_{i:c'_i=h} \mathcal{N}_p(y_i; \mu_h, \Sigma) \mathcal{N}_p(\mu_h; \mu_0, \kappa_0^{-1} \Sigma) d\mu_h IW(\Sigma; \nu_0, \Lambda_0) d\Sigma} < 0.$$

Hence from Theorem 1 all the data points would cluster together. \square

Proofs of Section 4

Proof of Lemma 1. Let (Λ_0, η_0) be the true parameters and Ψ be the partition induced by a given set of cluster labels $\{c_1, \dots, c_n\}$. Note that the oracle partition probability (11) is unchanged if $\boldsymbol{\eta}$ is multiplied by a full-rank square matrix. Hence if $\boldsymbol{\zeta}_0^{(p)} = \frac{1}{\sqrt{p}}(\Lambda_0^T \Lambda_0)^{\frac{1}{2}} \boldsymbol{\eta}_0$, then $\Pi(\Psi \mid \boldsymbol{\eta}_0) = \Pi(\Psi \mid \boldsymbol{\zeta}_0^{(p)})$. For all $i = 1, \dots, n$ the $\lim_{p \rightarrow \infty} p^{-1} \|\Lambda \eta_i - \Lambda_0 \eta_{0i}\| = 0$ implies that, for $p \rightarrow \infty$

$$p^{-1} \left| \eta_i^T \Lambda^T \Lambda \eta_i - \eta_{0i}^T \Lambda_0^T \Lambda_0 \eta_{0i} \right| = \left| \left\| \zeta_{0i}^{(p)} \right\|^2 - \left\| \zeta_i^{(p)} \right\|^2 \right| \rightarrow 0.$$

From Remark 1 we see that the numerator in the RHS of (11) can be written as

$$C \times \Pi(\Psi) \times \left| \sum_{h=1}^k \left\{ S_{\eta_0}^h + \frac{n_h}{n_h + 1} \bar{\eta}_0^h \bar{\eta}_0^{hT} \right\} \right|^{-\frac{n}{2}} \times \prod_{h=1}^k \left(\frac{\kappa_0}{n_h + \kappa_0} \right)^{\frac{d}{2}} \quad (\text{A.10})$$

where $n_h = \sum_{i=1}^n I(c_i = h)$, $\bar{\eta}_0^h = \frac{1}{n_h} \sum_{i:c_i=h} \eta_{0i}$, $S_{\eta_0}^h = \sum_{i:c_i=h} (\eta_{0i} - \bar{\eta}_0^h)(\eta_{0i} - \bar{\eta}_0^h)^T$ and C is a positive quantity constant across all $\Psi' \in \mathcal{P}$. Hence it is clear that $\Pi(\Psi \mid \boldsymbol{\zeta}_0^{(p)})$ is a continuous function of $\boldsymbol{\zeta}_0^{(p)}$. Therefore as $p \rightarrow \infty$

$$\begin{aligned} & \frac{1}{\sqrt{p}} \|\Lambda \eta_i - \Lambda_0 \eta_{0i}\| \rightarrow 0 \\ \Rightarrow & \left| \Pi(\Psi \mid \boldsymbol{\zeta}^{(p)}) - \Pi(\Psi \mid \boldsymbol{\zeta}_0^{(p)}) \right| \rightarrow 0 \Rightarrow \left| \Pi(\Psi \mid \boldsymbol{\zeta}^{(p)}) - \Pi(\Psi \mid \eta_0^{(p)}) \right| \rightarrow 0. \end{aligned} \quad (\text{A.11})$$

Now, the expectation of the posterior $E \left[\Pi(\Psi \mid \boldsymbol{\zeta}^{(p)}) \mid \mathbf{y} \right]$ can be decomposed into

$$\begin{aligned} E \left[\Pi(\Psi \mid \boldsymbol{\zeta}^{(p)}) \mid \mathbf{y} \right] &= E \left[\Pi(\Psi \mid \boldsymbol{\zeta}^{(p)}) \mid B_{p,\delta}, \mathbf{y} \right] \Pi(B_{p,\delta} \mid \mathbf{y}) \\ &\quad + E \left[\Pi(\Psi \mid \boldsymbol{\zeta}^{(p)}) \mid \bar{B}_{p,\delta}, \mathbf{y} \right] \Pi(\bar{B}_{p,\delta} \mid \mathbf{y}). \end{aligned} \quad (\text{A.12})$$

The second term in (A.12) goes to 0 as $\Pi(\bar{B}_{p,\delta} \mid \mathbf{y}) \rightarrow 0$ for $p \rightarrow \infty$ by assumption and $\Pi(\Psi \mid \boldsymbol{\zeta}^{(p)})$ is bounded. To conclude the proof note that $E \left[\Pi(\Psi \mid \boldsymbol{\zeta}^{(p)}) \mid B_{p,\delta}, \mathbf{y} \right] \rightarrow \Pi(\Psi \mid \eta_0)$ by (A.11) and the dominated convergence theorem. \square

Proof of Theorem 2. The proof follows along the lines of the proof of Theorem 6.39 of Ghosal and Van Der Vaart (2017). \square

Proof of Theorem 3. From Theorem 2 we see that Theorems 4-7, reported in the Supplementary Materials, directly imply the proof. Theorems 4 and 5 jointly imply condition (I). Theorem 6

implies condition (II) and lastly Theorem 7 implies condition (III). \square

REFERENCES

- Andrews, T. S. and Hemberg, M. (2018a), “Identifying Cell Populations with ScRNASeq,” *Molecular Aspects of Medicine*, 59, 114 – 122.
- (2018b), “M3Drop: Dropout-based Feature Selection for scRNASeq,” *Bioinformatics*, 35, 2865–2867.
- Azzalini, A. (2013), *The Skew-Normal and Related Families*, Institute of Mathematical Statistics Monographs, Cambridge University Press.
- Baglama, J. and Reichel, L. (2005), “Augmented Implicitly Restarted Lanczos Bidiagonalization Methods,” *SIAM Journal on Scientific Computing*, 27, 19–42.
- Banfield, J. D. and Raftery, A. E. (1993), “Model-Based Gaussian and Non-Gaussian Clustering,” *Biometrics*, 49, 803–821.
- Bhattacharya, A. and Dunson, D. B. (2011), “Sparse Bayesian Infinite Factor Models,” *Biometrika*, 98, 291–306.
- Bhattacharya, A., Pati, D., Pillai, N. S., and Dunson, D. B. (2015), “Dirichlet-Laplace Priors for Optimal Shrinkage,” *Journal of the American Statistical Association*, 110, 1479–1490.
- Bickel, P. J. and Levina, E. (2004), “Some Theory for Fisher’s Linear Discriminant Function, ‘naive Bayes’, and Some Alternatives When There Are Many More Variables Than Observations,” *Bernoulli*, 10, 989–1010.
- Bouveyron, C. and Brunet-Saumard, C. (2014), “Model-based Clustering of High-dimensional Data: A Review,” *Computational Statistics & Data Analysis*, 71, 52 – 78.
- Butler, A., Hoffman, P., Smibert, P., Papalexi, E., and Satija, R. (2018), “Integrating Single-Cell Transcriptomic Data Across Different Conditions, Technologies, and Species,” *Nature Biotechnology*, 36, 411–420.
- Cai, T. T., Ma, J., and Zhang, L. (2019), “CHIME: Clustering of High-Dimensional Gaussian Mixtures with EM Algorithm and Its Optimality,” *The Annals of Statistics*, 47, 1234–1267.

- Celeux, G. and Govaert, G. (1995), “Gaussian Parsimonious Clustering Models,” *Pattern Recognition*, 28, 781 – 793.
- Celeux, G., Kamary, K., Malsiner-Walli, G., Marin, J.-M., and Robert, C. P. (2018), “Computational Solutions for Bayesian Inference in Mixture Models,” in *Handbook of Mixture Analysis*, eds. Frühwirth-Schnatter, S., Celeux, G., and Robert, C. P., Boca Raton, FL: CRC Press, chap. 5, pp. 77–100.
- Corradin, R., Canale, A., and Nipoti, B. (2019), “BNPmix: Bayesian Nonparametric Mixture Models,” CRAN.
- Dunson, D. B. (2009), “Nonparametric Bayes Local Partition Models for Random Effects,” *Biometrika*, 96, 249–262.
- Dunson, D. B. and Johndrow, J. E. (2019), “The Hastings Algorithm at Fifty,” *Biometrika*, 107, 1–23.
- Eddelbuettel, D. and François, R. (2011), “Rcpp: Seamless R and C++ Integration,” *Journal of Statistical Software*, 40, 1–18.
- Escobar, M. D. and West, M. (1995), “Bayesian Density Estimation and Inference Using Mixtures,” *Journal of the American Statistical Association*, 90, 577–588.
- Fan, J., Fan, Y., and Lv, J. (2008), “High Dimensional Covariance Matrix Estimation Using a Factor Model,” *Journal of Econometrics*, 147, 186 – 197.
- Fan, J., Liao, Y., and Mincheva, M. (2011), “High-Dimensional Covariance Matrix Estimation in Approximate Factor Models,” *The Annals of Statistics*, 39, 3320–3356.
- Ferguson, T. S. (1973), “A Bayesian Analysis of Some Nonparametric Problems,” *Annals of Statistics*, 1, 209–230.
- Frühwirth-Schnatter, S. (2006), *Finite Mixture and Markov Switching Models*, Springer Science & Business Media.
- Galimberti, G. and Soffritti, G. (2013), “Using Conditional Independence for Parsimonious Model-Based Gaussian Clustering,” *Statistics and Computing*, 23, 625–638.

- George, E. I. and McCulloch, R. E. (1993), “Variable Selection via Gibbs Sampling,” *Journal of the American Statistical Association*, 88, 881–889.
- Ghahramani, Z., Hinton, G. E., et al. (1996), “The EM Algorithm for Mixtures of Factor Analyzers,” Tech. rep., Technical Report CRG-TR-96-1, University of Toronto.
- Ghosal, S. and Van Der Vaart, A. (2017), *Fundamentals of Nonparametric Bayesian Inference*, Cambridge Series in Statistical and Probabilistic Mathematics, Cambridge University Press.
- Gilks, W. R., Richardson, S., and Spiegelhalter, D. J. (1996), *Markov Chain Monte Carlo in Practice*, London: Chapman and Hall.
- Jain, S. and Neal, R. M. (2004), “A Split-Merge Markov Chain Monte Carlo Procedure for the Dirichlet Process Mixture Model,” *Journal of Computational and Graphical Statistics*, 13, 158–182.
- Jefferys, W. H. and Berger, J. O. (1992), “Ockham’s Razor and Bayesian Analysis,” *American Scientist*, 80, 64–72.
- Kim, S., Tadesse, M. G., and Vannucci, M. (2006), “Variable Selection in Clustering via Dirichlet Process Mixture Models,” *Biometrika*, 93, 877–893.
- Kingma, D. P., Mohamed, S., Jimenez Rezende, D., and Welling, M. (2014), “Semi-supervised Learning with Deep Generative Models,” in *Advances in Neural Information Processing Systems 27*, eds. Ghahramani, Z., Welling, M., Cortes, C., Lawrence, N. D., and Weinberger, K. Q., Curran Associates, Inc., pp. 3581–3589.
- Legramanti, S., Durante, D., and Dunson, D. B. (2020), “Bayesian Cumulative Shrinkage for Infinite Factorizations,” *Biometrika*.
- Li, H., Courtois, E. T., Sengupta, D., Tan, Y., Chen, K. H., Goh, J. J. L., Kong, S. L., Chua, C., Hon, L. K., Tan, W. S., et al. (2017), “Reference Component Analysis of Single-Cell Transcriptomes Elucidates Cellular Heterogeneity in Human Colorectal Tumors,” *Nature Genetics*, 49, 708.
- Lock, E. F. and Dunson, D. B. (2013), “Bayesian Consensus Clustering,” *Bioinformatics*, 29, 2610–2616.

- Lun, A. T., Bach, K., and Marioni, J. C. (2016), “Pooling Across Cells to Normalize Single-Cell RNA Sequencing Data with Many Zero Counts,” *Genome Biology*, 17, 75.
- McInnes, L., Healy, J., and Melville, J. (2018), “UMAP: Uniform Manifold Approximation and Projection for Dimension Reduction,” *arXiv preprint arXiv:1802.03426*.
- Miller, J. W. and Dunson, D. B. (2019), “Robust Bayesian Inference via Coarsening,” *Journal of the American Statistical Association*, 114, 1113–1125, PMID: 31942084.
- Miller, J. W. and Harrison, M. T. (2018), “Mixture Models with a Prior on the Number of Components,” *Journal of the American Statistical Association*, 113, 340–356.
- Murphy, K., Viroli, C., and Gormley, I. C. (2019), *IMIFA: Infinite Mixtures of Infinite Factor Analysers and Related Models*, R package version 2.1.1.
- Neal, R. M. (2000), “Markov Chain Sampling Methods for Dirichlet Process Mixture Models,” *Journal of Computational and Graphical Statistics*, 9, 249–265.
- Pati, D., Bhattacharya, A., Pillai, N. S., and Dunson, D. (2014), “Posterior Contraction in Sparse Bayesian Factor Models for Massive Covariance Matrices,” *The Annals of Statistics*, 42, 1102–1130.
- Pitman, J. and Yor, M. (1997), “The Two-Parameter Poisson-Dirichlet Distribution Derived from a Stable Subordinator,” *Annals of Probability*, 25, 855–900.
- Rand, W. M. (1971), “Objective Criteria for the Evaluation of Clustering Methods,” *Journal of the American Statistical Association*, 66, 846–850.
- Rezende, D. J., Mohamed, S., and Wierstra, D. (2014), “Stochastic Backpropagation and Approximate Inference in Deep Generative Models,” *arXiv preprint arXiv:1401.4082*.
- Richardson, S. and Green, P. J. (1997), “On Bayesian Analysis of Mixtures with an Unknown Number of Components (with Discussion),” *Journal of the Royal Statistical Society: Series B (Statistical Methodology)*, 59, 731–792.
- Rousseeuw, P. J. (1987), “Silhouettes: A Graphical Aid to the Interpretation and Validation of Cluster Analysis,” *Journal of Computational and Applied Mathematics*, 20, 53 – 65.

- Rudelson, M. and Vershynin, R. (2013), “Hanson-Wright Inequality and Sub-Gaussian Concentration,” *Electron. Commun. Probab.*, 18, 9 pp.
- Scott, S. L., Blocker, A. W., Bonassi, F. V., Chipman, H. A., George, E. I., and McCulloch, R. E. (2016), “Bayes and Big Data: The Consensus Monte Carlo Algorithm,” *International Journal of Management Science and Engineering Management*, 11, 78–88.
- Scrucca, L., Fop, M., Murphy, T. B., and Raftery, A. E. (2016), “Mclust 5: Clustering, Classification and Density Estimation Using Gaussian Finite Mixture Models,” *The R Journal*, 8, 289.
- See, P., Lum, J., Chen, J., and Ginhoux, F. (2018), “A Single-Cell Sequencing Guide for Immunologists,” *Frontiers in Immunology*, 9, 2425.
- Tadesse, M. G., Sha, N., and Vannucci, M. (2005), “Bayesian Variable Selection in Clustering High-Dimensional Data,” *Journal of the American Statistical Association*, 100, 602–617.
- Valdes-Mora, F., Handler, K., Law, A. M. K., Salomon, R., Oakes, S. R., Ormandy, C. J., and Gallego-Ortega, D. (2018), “Single-Cell Transcriptomics in Cancer Immunobiology: The Future of Precision Oncology,” *Frontiers in Immunology*, 9, 2582.
- Vershynin, R. (2012), *Introduction to the Non-Asymptotic Analysis of Random Matrices*, Cambridge University Press, pp. 210–268.
- Wade, S. and Ghahramani, Z. (2018), “Bayesian Cluster Analysis: Point Estimation and Credible Balls (with Discussion),” *Bayesian Analysis*, 13, 559–626.
- Wang, X. and Dunson, D. B. (2013), “Parallelizing MCMC via Weierstrass Sampler,” *arXiv preprint arXiv:1312.4605*.
- Zou, H., Hastie, T., and Tibshirani, R. (2006), “Sparse Principal Component Analysis,” *Journal of Computational and Graphical Statistics*, 15, 265–286.

A. SUPPLEMENTARY MATERIAL

A.1 Additional theoretical results

Lemma 2. *For prior (7) $\lim_{p \rightarrow \infty} \frac{1}{p} \lambda_{\min}(\Lambda^T \Lambda) = \lim_{p \rightarrow \infty} \frac{1}{p} \lambda_{\max}(\Lambda^T \Lambda) = v_1$ for some $v_1 > 0$ Π -a.s.*

Proof. Note that $\Lambda^T \Lambda = \tau^2 T^T T$ where the (i, j) -th element of T is $t_{ij} = e_{ij} \phi_{ij}$ with $e_{ij} \stackrel{iid}{\sim} \text{DE}(1)$. Also, $\phi \sim \text{Dir}(a, \dots, a)$ and $\tau \sim \text{Ga}(pda, 1/2)$. Therefore,

$$\tau \stackrel{d}{=} \sum_{i=1}^p \sum_{j=1}^d \tau_{ij}, \quad \phi \stackrel{d}{=} \frac{1}{\sum_{i=1}^p \sum_{j=1}^d \gamma_{ij}} (\gamma_{11}, \dots, \gamma_{pd}),$$

where $\gamma_{ij} \stackrel{iid}{\sim} \text{Ga}(a, 1/2)$ and $\tau_{ij} \stackrel{iid}{\sim} \text{Ga}(a, 1/2)$. Therefore T can be written as $T = \Gamma^{-1} \tilde{T}$ where $\tilde{t}_{ij} = e_{ij} \gamma_{ij}$ and $\Gamma = \sum_{i=1}^p \sum_{j=1}^d \gamma_{ij}$. Thus

$$\lambda_i(\Lambda^T \Lambda) = \left(\frac{\tau}{\Gamma} \right)^2 \times \lambda_i(\tilde{T}^T \tilde{T}) \text{ for any } i = 1, \dots, p.$$

Now by the strong law of large numbers $\left\| \frac{1}{p} \tilde{T}^T \tilde{T} - v_1 I_d \right\|_F \rightarrow 0$ as $p \rightarrow \infty$ where $\|\cdot\|_F$ is the Frobenius norm of a matrix and $v_1 = \text{Var}(e_{ij} \gamma_{ij})$. Hence, for any $i = 1, \dots, p$ $\lim_{p \rightarrow \infty} \lambda_i(\tilde{T}^T \tilde{T}) p^{-1} = v_1$. Also $\lim_{p \rightarrow \infty} \tau/(pd) = E(\tau_{ij})$ which implies that $\lim_{p \rightarrow \infty} (\tau/\Gamma)^2 = 1$ Π -a.s. Hence the proof. \square

Theorem 4. *For any $\epsilon > 0$ define $B_p^\epsilon = \{\Theta : KL(\mathbb{P}_0^p, \mathbb{P}_\Theta^p) p^{-1} \leq \epsilon\}$. Then, under the settings of Section 4, $\liminf \Pi(B_p^\epsilon) > 0$.*

Proof. Let P_0 and P be p -variate multivariate normal distributions with $P = \mathcal{N}_p(\mu, \Sigma)$ and $P_0 = \mathcal{N}_p(\mu_0, \Sigma_0)$. Then their Kullback-Leibler divergence is

$$KL(P_0, P) = \frac{1}{2} \left[\log \frac{|\Sigma|}{|\Sigma_0|} + \text{tr}(\Sigma^{-1} \Sigma_0) + (\mu - \mu_0)^T \Sigma^{-1} (\mu - \mu_0) - p \right],$$

which, under the settings of Section 4, simplifies to

$$KL(\mathbb{P}_0^p, \mathbb{P}_\Theta^p) = \frac{1}{2} \left[np \log \frac{\sigma^2}{\sigma_0^2} + np \left(\frac{\sigma_0^2}{\sigma^2} - 1 \right) + \frac{1}{\sigma^2} \sum_{i=1}^n (\mu_i - \mu_{0i})^T (\mu_i - \mu_{0i}) \right], \quad (\text{A.13})$$

where $\mu_i = \Lambda \eta_i$ and $\mu_{0i} = \Lambda_0 \eta_{0i}$. Now,

$$\begin{aligned} \Pi \left\{ KL(\mathbb{P}_0^p, \mathbb{P}_\theta^p) p^{-1} < \epsilon \right\} &= \Pi \left\{ \left[n \log \frac{\sigma^2}{\sigma_0^2} + n \left(\frac{\sigma_0^2}{\sigma^2} - 1 \right) + \frac{1}{p\sigma^2} \sum_{i=1}^n (\mu_i - \mu_{0i})^T (\mu_i - \mu_{0i}) \right] < \epsilon \right\} \\ &\geq \Pi \left\{ \log \frac{\sigma^2}{\sigma_0^2} + \left(\frac{\sigma_0^2}{\sigma^2} - 1 \right) \leq \frac{\epsilon}{2n}, \frac{1}{\sigma^2} \sum_{i=1}^n (\mu_i - \mu_{0i})^T (\mu_i - \mu_{0i}) < \frac{p\epsilon}{2} \right\}. \end{aligned}$$

Note that for any $x > 0$ $\log x \leq x - 1$ and therefore $\log \frac{\sigma^2}{\sigma_0^2} + \left(\frac{\sigma_0^2}{\sigma^2} - 1 \right) \leq \left(\frac{\sigma_0}{\sigma} - \frac{\sigma}{\sigma_0} \right)^2$ implying that

$$\begin{aligned} \Pi \left\{ KL(\mathbb{P}_0^p, \mathbb{P}_\theta^p) p^{-1} < \epsilon \right\} &\geq \Pi \left\{ \left(\frac{\sigma_0}{\sigma} - \frac{\sigma}{\sigma_0} \right)^2 \leq \frac{\epsilon}{2n}, \frac{1}{\sigma^2} \sum_{i=1}^n (\mu_i - \mu_{0i})^T (\mu_i - \mu_{0i}) < \frac{p\epsilon}{2} \right\} \\ &\geq \Pi \left\{ \left(\frac{\sigma_0}{\sigma} - \frac{\sigma}{\sigma_0} \right)^2 \leq \frac{\epsilon}{2n} \right\} \Pi \left\{ \sum_{i=1}^n (\mu_i - \mu_{0i})^T (\mu_i - \mu_{0i}) < \sigma_L \frac{p\epsilon}{2} \right\}, \end{aligned}$$

where the second inequality holds thanks to condition (C3). The first factor above is positive under our proposed prior on σ . Now consider the second factor and note that for each $i = 1, \dots, n$

$$(\mu_i - \mu_{0i})^T (\mu_i - \mu_{0i}) = \left\| \Lambda(\eta_i - (\Lambda^T \Lambda)^{-1} \Lambda^T \Lambda_0 \eta_{0i}) \right\|^2 + \eta_{0i}^T (\Lambda_0^T \Lambda_0 - \Lambda_0^T \Lambda (\Lambda^T \Lambda)^{-1} \Lambda^T \Lambda_0) \eta_{0i}.$$

By the triangle inequality

$$\frac{1}{p} \left\| \Lambda_0^T \Lambda_0 - \Lambda_0^T \Lambda (\Lambda^T \Lambda)^{-1} \Lambda^T \Lambda_0 \right\|_2 \leq \left\| \frac{1}{p} \Lambda_0^T \Lambda_0 - v_0 I_d \right\|_2 + \left\| v_0 I_d - \frac{1}{p} \Lambda_0^T \Lambda (\Lambda^T \Lambda)^{-1} \Lambda^T \Lambda_0 \right\|_2. \quad (\text{A.14})$$

The first term on the right hand side of (A.14) goes to 0 as $p \rightarrow \infty$ by (C2). Let us define the matrix $B = (\Lambda^T \Lambda)^{-1/2} \Lambda^T$, with $\|B\|_2 = 1$. From Vershynin (2012, Theorem 5.39) it follows that for any $0 < \epsilon < 1$ and large enough p

$$\sqrt{v_0} - \epsilon \leq \left\| \frac{1}{\sqrt{p}} \Lambda_0 \right\|_2 \leq \sqrt{v_0} + \epsilon.$$

From Lemma 1.1 of the Supplement section of Pati et al. (2014) we have that

$$\sqrt{v_0} - \epsilon \leq \left\| \frac{1}{\sqrt{p}} B \Lambda_0 \right\|_2 \leq \sqrt{v_0} + \epsilon, \quad \sqrt{v_0} - \epsilon \leq \frac{1}{\sqrt{p}} s_{\min}(B \Lambda_0) \leq \sqrt{v_0} + \epsilon.$$

Therefore $\lim_{p \rightarrow \infty} \lambda_i (\Lambda_0^T \Lambda (\Lambda^T \Lambda)^{-1} \Lambda^T \Lambda_0) p^{-1} = v_0$ for all $i = 1, \dots, d$. Hence the second term on the right hand side of (A.14) goes to 0 as $p \rightarrow \infty$ and therefore $\lim_{p \rightarrow \infty} \frac{1}{p} \eta_{0i}^T (\Lambda_0^T \Lambda_0 - \Lambda_0^T \Lambda (\Lambda^T \Lambda)^{-1} \Lambda^T \Lambda_0) \eta_{0i} = 0$ for all $i = 1, \dots, n$. Now (C2) and Lemma 2 jointly imply that $\|(\Lambda^T \Lambda)^{-1} \Lambda^T \Lambda_0\|_2 = O(1)$ Π -a.s. Therefore, for standard normal priors on the latent variables,

$$\liminf_{p \rightarrow \infty} \Pi \left\{ \sum_{i=1}^n (\mu_i - \mu_{0i})^T (\mu_i - \mu_{0i}) < \sigma_L p \epsilon \right\} > 0.$$

From the permanence of KL-property of mixture priors (Ghosal and Van Der Vaart 2017, Proposition 6.28) we can conclude that the right hand side is also positive. \square

Theorem 5. *On the set B_p^ϵ defined in Theorem 4 for $r = 2$ we have*

$$V_r^+(\mathbb{P}_0^p, \mathbb{P}_\vartheta^p) = o(p^r).$$

Proof. For $r = 2$

$$V_r^+(\mathbb{P}_0^p, \mathbb{P}_\vartheta^p) \leq \int \log^2 \frac{p_0^p}{p_\vartheta^p} d\mathbb{P}_0^p - \left\{ \int \log \frac{p_0^p}{p_\vartheta^p} d\mathbb{P}_0^p \right\}^2.$$

Now conditionally on $\vartheta \in \vartheta$, the observations y_1, \dots, y_n are independent. Therefore,

$$V_r^+(\mathbb{P}_0^p, \mathbb{P}_\vartheta^p) \leq \sum_{j=1}^n \left[\int \log^2 \frac{p_{0j}(y_j)}{p_{\vartheta j}(y_j)} p_{0j}(y_j) dy_j - \left\{ \int \log \frac{p_{0j}(y_j)}{p_{\vartheta j}(y_j)} p_{0j}(y_j) dy_j \right\}^2 \right] \quad (\text{A.15})$$

where $p_{0j}(y_j) = \prod_{i=1}^p \mathcal{N}(y_{ji}; \mu_{0ji}, \sigma_0^2)$ and $p_{\vartheta j}(y_j) = \prod_{i=1}^p \mathcal{N}(y_{ji}; \mu_{ji}, \sigma^2)$ with $\mu_{0j} =$ and $\mu_j = \Lambda \eta_j$. We first show the result for a particular term inside the summation of (A.15). Since $\|\eta_{0i}\| = O(1)$ and n is fixed, the result will readily follow afterwards. For simplicity, we drop the suffix j from the terms of (A.15) henceforth. Consider,

$$\begin{aligned} \log^2 \frac{p_0(y_i)}{p_\vartheta(y_i)} &= \left[\log \frac{\sigma}{\sigma_0} - \frac{1}{2} \left\{ \left(\frac{y_i - \mu_{0i}}{\sigma_0} \right)^2 - \left(\frac{y_i - \mu_i}{\sigma} \right)^2 \right\} \right]^2 \\ &= \frac{1}{4} \left\{ \left(\frac{y_i - \mu_{0i}}{\sigma_0} \right)^2 - \left(\frac{y_i - \mu_i}{\sigma} \right)^2 \right\}^2 + \log^2 \frac{\sigma}{\sigma_0} - \left\{ \left(\frac{y_i - \mu_{0i}}{\sigma_0} \right)^2 - \left(\frac{y_i - \mu_i}{\sigma} \right)^2 \right\} \log \frac{\sigma}{\sigma_0}. \end{aligned}$$

Note that,

$$\begin{aligned} \left\{ \left(\frac{y_i - \mu_{0i}}{\sigma_0} \right)^2 - \left(\frac{y_i - \mu_i}{\sigma} \right)^2 \right\}^2 &= \left\{ z_i^2 \left(1 - \frac{\sigma_0^2}{\sigma^2} \right) - 2z_i(\mu_{0i} - \mu_i) \frac{\sigma_0}{\sigma} + \left(\frac{\mu_i - \mu_{0i}}{\sigma} \right)^2 \right\}^2 \\ &= z_i^4 \left(1 - \frac{\sigma_0^2}{\sigma^2} \right)^2 + 4z_i^2 \sigma_0^2 \left(\frac{\mu_{0i} - \mu_i}{\sigma} \right)^2 + \left(\frac{\mu_i - \mu_{0i}}{\sigma} \right)^4 - 2z_i^3 \left(1 - \frac{\sigma_0^2}{\sigma^2} \right) \frac{\sigma_0}{\sigma} (\mu_{0i} - \mu_i) \\ &\quad - 2z_i \sigma_0 \left(\frac{\mu_{0i} - \mu_i}{\sigma} \right)^3 + 2z_i^2 \left(\frac{\mu_{0i} - \mu_i}{\sigma} \right)^2 \left(1 - \frac{\sigma_0^2}{\sigma^2} \right) \end{aligned}$$

where $z_i = (y_i - \mu_{0i})/\sigma_0$ and $z_i \stackrel{iid}{\sim} \mathcal{N}(0, 1)$. Therefore,

$$E_{y_i} \left\{ \left(\frac{y_i - \mu_{0i}}{\sigma_0} \right)^2 - \left(\frac{y_i - \mu_i}{\sigma} \right)^2 \right\} = \left(1 - \frac{\sigma_0^2}{\sigma^2} \right) + \left(\frac{\mu_i - \mu_{0i}}{\sigma} \right)^2 \text{ and}$$

$$\begin{aligned} E_{y_i} \left\{ \left(\frac{y_i - \mu_{0i}}{\sigma_0} \right)^2 - \left(\frac{y_i - \mu_i}{\sigma} \right)^2 \right\}^2 &= 3 \left(1 - \frac{\sigma_0^2}{\sigma^2} \right)^2 + 4\sigma_0^2 \left(\frac{\mu_{0i} - \mu_i}{\sigma} \right)^2 + \left(\frac{\mu_i - \mu_{0i}}{\sigma} \right)^4 \\ &\quad + 2 \left(\frac{\mu_{0i} - \mu_i}{\sigma} \right)^2 \left(1 - \frac{\sigma_0^2}{\sigma^2} \right). \end{aligned}$$

Hence,

$$\begin{aligned} \int \left\{ \log \frac{p_0(y_i)}{p_\vartheta(y_i)} \right\}^2 p_0(y_i) dy_i &= \left(\frac{\mu_{0i} - \mu_i}{\sigma} \right)^2 \times \left\{ \sigma_0^2 + \frac{1}{2} \left(1 - \frac{\sigma_0^2}{\sigma^2} \right) - \log \frac{\sigma}{\sigma_0} \right\} \\ &\quad - \log \frac{\sigma}{\sigma_0} \left(1 - \frac{\sigma_0^2}{\sigma^2} \right) + \frac{1}{4} \left(\frac{\mu_{0i} - \mu_i}{\sigma} \right)^4 + \frac{3}{4} \left(1 - \frac{\sigma_0^2}{\sigma^2} \right)^2 + \log^2 \frac{\sigma}{\sigma_0} \end{aligned}$$

$$\begin{aligned} \left\{ \int \log \frac{p_0(y_i)}{p_\vartheta(y_i)} p_0(y_i) dy_i \right\}^2 &= \left\{ \log \frac{\sigma}{\sigma_0} + \frac{\sigma_0^2 + (\mu_{0i} - \mu_i)^2}{2\sigma^2} - \frac{1}{2} \right\}^2 = \log^2 \frac{\sigma}{\sigma_0} + \frac{1}{4} \left(1 - \frac{\sigma_0^2}{\sigma^2} \right)^2 \\ &\quad + \frac{1}{4} \left(\frac{\mu_{0i} - \mu_i}{\sigma} \right)^4 + \left(\frac{\mu_{0i} - \mu_i}{\sigma} \right)^2 \times \left\{ \log \frac{\sigma}{\sigma_0} - \frac{1}{2} \left(1 - \frac{\sigma_0^2}{\sigma^2} \right) \right\} - \log \frac{\sigma}{\sigma_0} \left(1 - \frac{\sigma_0^2}{\sigma^2} \right), \end{aligned}$$

leading to

$$\begin{aligned} V_r^+(\mathbb{P}_0^p, \mathbb{P}_\vartheta^p) &\leq \sum_{i=1}^p \left[\int \left\{ \log \frac{p_0(y_i)}{p_\vartheta(y_i)} \right\}^2 p_0(y_i) dy_i - \left\{ \int \log \frac{p_0(y_i)}{p_\vartheta(y_i)} p_0(y_i) dy_i \right\}^2 \right] \\ &= \frac{p}{2} \left(1 - \frac{\sigma_0^2}{\sigma^2} \right)^2 + \left\{ \sigma_0^2 - 2 \log \frac{\sigma}{\sigma_0} + \left(1 - \frac{\sigma_0^2}{\sigma^2} \right) \right\} \times \sum_{i=1}^p \left(\frac{\mu_{0i} - \mu_i}{\sigma} \right)^2. \end{aligned} \quad (\text{A.16})$$

Note that

$$\sum_{i=1}^p (\mu_{0i} - \mu_i)^2 = \sum_{i=1}^p \left(\lambda_{0i}^T \eta_0 - \lambda_i^T \eta \right)^2 = \eta_0^T \Lambda_0^T \Lambda_0 \eta_0 + \eta^T \Lambda^T \Lambda \eta - 2 \eta_0^T \Lambda_0^T \Lambda \eta. \quad (\text{A.17})$$

Now $\eta_0^T \Lambda_0^T \Lambda_0 \eta_0 \leq \|\Lambda_0\|_2^2 \|\eta_0\|^2$ and therefore, by conditions (C2) and (C4), $\eta_0^T \Lambda_0^T \Lambda_0 \eta_0 = O(p)$. Also from Lemma 2, $\frac{1}{p} \|\Lambda\|_2^2 \leq c$ for large enough p and some $c > 0$ and therefore $\eta^T \Lambda^T \Lambda \eta \leq \|\Lambda\|_2^2 \|\eta\|^2 = \|\eta\|^2 O(p)$. From the proof of Theorem 4 we can see that in the set B_p^ϵ , $\|\eta\|$ is bounded. We have shown that the highest powers in (A.17) and thus in (A.16) are almost surely bounded by p for large enough p . Hence the proof. \square

Theorem 6. *Let us define the test function $\phi_p = \mathbb{1} \left\{ \left| \frac{1}{\sqrt{np}\sigma_0} \left\| \sum_{i=1}^n (Y_i - \Lambda_0 \eta_{0i}) \right\| - 1 \right| > \tau_{np} \right\}$ to test the following hypothesis $H_0 : Y_1, \dots, Y_n \sim \mathbb{P}_0^p$ versus $H_1 : H_0$ is false where τ_{np} is a positive real number. Define the set $\tilde{\Theta}_p = \bar{B}_{p,\delta}$. Then there exists a constant $C > 0$ such that*

$$\phi_p \rightarrow 0 \text{ } \mathbb{P}_0^p\text{-a.s.}; \quad \int_{\tilde{\Theta}_p} \mathbb{P}_\vartheta^p(1 - \phi_p) d\Pi(\vartheta) \leq e^{-Cp}.$$

Proof. Let us define $\mu_i = \Lambda \eta_i$ and $\mu_{0i} = \Lambda \eta_{0i}$. Then under H_0 , $\frac{1}{\sqrt{n}\sigma_0} \sum_{i=1}^n (y_i - \Lambda \eta_{0i}) \sim \mathcal{N}_p(0, I_p)$ and therefore $\frac{1}{\sqrt{np}\sigma_0} \sum_{i=1}^n (y_i - \Lambda \eta_{0i}) \stackrel{d}{=} \omega / \sqrt{p}$ where $\omega \sim \mathcal{N}_p(0, I_p)$. Then from Rudelson and Vershynin (2013, Theorem 2.1) for some $c > 0$ and any $\tau_{np} > 0$

$$\mathbb{P}_0^p \phi_p = \Pr \left[\left| \frac{1}{\sqrt{p}} \|\omega\| - 1 \right| > \tau_{np} \right] \leq 2 \exp \left(-pc\tau_{np}^2 \right)$$

Since $\sum_{p=1}^\infty \mathbb{P}_0^p \phi_p < \infty$, by Borel-Cantelli lemma $\phi_p \rightarrow 0$ \mathbb{P}_0^p -a.s.

Notably when H_0 is not true i.e. under \mathbb{P}_ϑ^p , $Y_i \stackrel{d}{=} \sigma \varphi_i + \Lambda \eta_i$ where $\varphi_i \stackrel{\text{iid}}{\sim} \mathcal{N}_p(0, I_p)$ for some

$\vartheta \neq (\Lambda_0, \eta_0, \sigma_0)$ and therefore under \mathbb{P}_ϑ^p

$$\mathbb{P}_\vartheta^p(1 - \phi_p) \leq \mathbb{P}_\vartheta^p \left[\frac{1}{\sqrt{np}\sigma} \left\| \sum_{i=1}^n (y_i - \Lambda\eta_i) \right\| < \frac{\sigma_0}{\sigma} \left(\frac{1}{\sqrt{np}\sigma_0} \sum_{i=1}^n \|\Lambda\eta_i - \Lambda\eta_{0i}\| + 1 + \tau_{np} \right) \right].$$

Again under \mathbb{P}_ϑ^p , $\frac{1}{\sqrt{np}\sigma} \sum_{i=1}^n (y_i - \Lambda\eta_i) \stackrel{d}{=} \omega/\sqrt{p}$ and hence $\|\omega\| = \sqrt{\sum_{j=1}^p \omega_j^2} \geq \sqrt{p}\bar{\omega}$ where $\bar{\omega} = \frac{1}{p} \sum_{j=1}^p \omega_j$. Hence $\mathbb{P}_\vartheta^p(1 - \phi_p) \leq \Pr[\bar{\omega} < C_p]$ where $C_p = \frac{\sigma_0}{\sigma} \left(\frac{1}{\sqrt{np}\sigma_0} \sum_{i=1}^n \|\Lambda\eta_i - \Lambda\eta_{0i}\| + 1 + \tau_{np} \right)$. Note that for $\vartheta \in \tilde{\Theta}_p$, $\liminf C_p > 0$ and thus $\Pr(\bar{\omega} < C_p) < 2 \exp(-pC_p^2/2)$. Hence the proof. \square

Theorem 7. Let $\tilde{\Pi}_p$ be the renormalized restriction of Π to the set B_p^ϵ defined in Theorem 4. Then $\mathbb{1}\{\bar{A}_p\} \rightarrow 0$ \mathbb{P}_0^p -a.s.

Proof. If we can show that $\sum_{p=1}^\infty \mathbb{P}_0^p(\bar{A}_p) < \infty$, then by Borel-Cantelli lemma $\mathbb{P}_0^p[\limsup \bar{A}_p] = 0$ and henceforth $\mathbb{1}\{\bar{A}_p\} \rightarrow 0$ \mathbb{P}_0^p -a.s. Now

$$\mathbb{P}_0^p(\bar{A}_p) = \mathbb{P}_0^p \left[\frac{1}{p} \int \sum_{i=1}^n \left\{ \frac{1}{\sigma^2} \|y_i - \mu_i\|^2 - \frac{1}{\sigma_0^2} \|y_i - \mu_{0i}\|^2 - \frac{1}{\sigma^2} \|\mu_i - \mu_{0i}\|^2 - p \left(\frac{\sigma_0^2}{\sigma^2} - 1 \right) \right\} d\tilde{\Pi}_p > 2\epsilon \right].$$

Notably under \mathbb{P}_0^p , $Y_i \stackrel{d}{=} \sigma_0\varphi_i + \mu_{0i}$ where $\varphi_i \stackrel{\text{iid}}{\sim} \mathcal{N}_p(0, I_p)$. Therefore

$$\begin{aligned} \mathbb{P}_0^p(\bar{A}_p) &= \Pr \left[\frac{1}{p} \int \sum_{i=1}^n \left\{ \left(\frac{\sigma_0^2}{\sigma^2} - 1 \right) (\|\varphi_i\|^2 - p) + 2 \frac{\sigma_0}{\sigma^2} \varphi_i^T (\mu_i - \mu_{0i}) \right\} d\tilde{\Pi}_p > 2\epsilon \right] \\ &\leq \Pr \left[\frac{1}{p} \sum_{i=1}^n (\|\varphi_i\|^2 - p) \int \left(\frac{\sigma_0^2}{\sigma^2} - 1 \right) d\tilde{\Pi}_p > \tilde{\epsilon} \right] + \Pr \left[\frac{2}{p} \int \sum_{i=1}^n \left\{ \frac{\sigma_0}{\sigma^2} \varphi_i^T (\mu_i - \mu_{0i}) \right\} d\tilde{\Pi}_p > \tilde{\epsilon} \right]. \end{aligned} \tag{A.18}$$

Let us consider the first term of (A.18). Notably

$$\Pr \left[\frac{1}{p} \sum_{i=1}^n (\|\varphi_i\|^2 - p) \int \left(\frac{\sigma_0^2}{\sigma^2} - 1 \right) d\tilde{\Pi}_p > \tilde{\epsilon} \right] \leq \Pr \left[\frac{1}{p} \left| \sum_{i=1}^n (\|\varphi_i\|^2 - p) \right| \times \int \left| \frac{\sigma_0^2}{\sigma^2} - 1 \right| d\tilde{\Pi}_p > \tilde{\epsilon} \right]. \tag{A.19}$$

From (C3) we have that σ lies in a compact interval. Hence the integral in the right hand side

of (A.19) is bounded above by some positive constant, say $C_{\sigma,1}$. Therefore,

$$\Pr \left[\frac{1}{p} \sum_{i=1}^n (\|\varphi_i\|^2 - p) \int \left(\frac{\sigma_0^2}{\sigma^2} - 1 \right) d\tilde{\Pi}_p > \tilde{\epsilon} \right] \leq \Pr \left[\frac{1}{p} \left| \sum_{i=1}^n (\|\varphi_i\|^2 - p) \right| > \frac{\tilde{\epsilon}}{C_{\sigma,1}} \right] \leq 2e^{-pC_{\sigma,2}}.$$

for some positive constant $C_{\sigma,2} > 0$. The second inequality in the above equation follows from Rudelson and Vershynin (2013, Theorem 1.1). Clearly

$$\sum_{p=1}^{\infty} \Pr \left[\frac{1}{p} \sum_{i=1}^n (\|\varphi_i\|^2 - p) \int \left(\frac{\sigma_0^2}{\sigma^2} - 1 \right) d\tilde{\Pi}_p > \tilde{\epsilon} \right] < \infty. \quad (\text{A.20})$$

Now we consider the second term of (A.18). As $\varphi_i = (\varphi_{i1}, \dots, \varphi_{ip})^T$ (similarly μ_i and μ_{0i} are also p -dimensional vectors) we can write

$$\begin{aligned} \Pr \left[\frac{2}{p} \int \sum_{i=1}^n \left\{ \frac{\sigma_0}{\sigma^2} \varphi_i^T (\mu_i - \mu_{0i}) \right\} d\tilde{\Pi}_p > \tilde{\epsilon} \right] &= \Pr \left[\frac{2}{p} \sum_{i=1}^n \sum_{j=1}^p \varphi_{ij} \int \left\{ \frac{\sigma_0}{\sigma^2} (\mu_{ij} - \mu_{0ij}) \right\} d\tilde{\Pi}_p > \tilde{\epsilon} \right] \\ &\leq \exp \left[- \frac{p^2 \tilde{\epsilon}^2}{4\sigma_0^2 \sum_{i=1}^n \sum_{j=1}^p E_{\tilde{\Pi}_p}^2 \left\{ \frac{1}{\sigma^2} (\mu_{ij} - \mu_{0ij}) \right\}} \right], \end{aligned}$$

where $E_{\tilde{\Pi}_p}$ denotes the expectation with respect to the probability measure $\tilde{\Pi}_p$. The above inequality follows from sub-Gaussian concentration bounds. Now

$$\begin{aligned} \sum_{i=1}^n \sum_{j=1}^p E_{\tilde{\Pi}_p}^2 \left\{ \frac{1}{\sigma^2} (\mu_{ij} - \mu_{0ij}) \right\} &\leq \sum_{i=1}^n E_{\tilde{\Pi}_p} \frac{1}{\sigma^4} \|\mu_i - \mu_{0i}\|^2 \quad (\text{by Jensen's inequality}) \\ &= E_{\tilde{\Pi}_p} \frac{1}{\sigma^4} \sum_{i=1}^n \|\mu_i - \mu_{0i}\|^2. \end{aligned} \quad (\text{A.21})$$

Since we consider independent priors on σ, Λ and η_i , (A.21) follows from its preceding step.

Note that on the set B_p^ϵ

$$n \log \frac{\sigma^2}{\sigma_0^2} + n \left(\frac{\sigma_0^2}{\sigma^2} - 1 \right) + \frac{1}{p\sigma^2} \sum_{i=1}^n \|\mu_i - \mu_{0i}\|^2 < 2\epsilon. \quad (\text{A.22})$$

From the inequality $\log x < x - 1$ we see that $n \log \frac{\sigma^2}{\sigma_0^2} + n \left(\frac{\sigma_0^2}{\sigma^2} - 1 \right) > 0$. Therefore for $\vartheta \in B_p^\epsilon$, in conjunction of (A.22) and (C3) we have $\frac{1}{p} \sum_{i=1}^n \|\mu_i - \mu_{0i}\|^2 < 2\epsilon\sigma_U^2 \Rightarrow \frac{1}{p} \sum_{i=1}^n E_{\tilde{\Pi}_p} \|\mu_i - \mu_{0i}\|^2 < 2\epsilon\sigma_U^2$. Also thanks to (C3) $E_{\tilde{\Pi}_p} \frac{1}{\sigma^4}$ is bounded above. Hence the term in (A.21) is bounded above

and consequently

$$\sum_{p=1}^{\infty} \Pr \left[\frac{2}{p} \int \sum_{i=1}^n \left\{ \frac{\sigma_0}{\sigma^2} \varphi_i^T(\mu_i - \mu_{0i}) \right\} d\tilde{\Pi}_p > \tilde{\epsilon} \right] < \infty. \quad (\text{A.23})$$

Combining (A.20) and (A.23) we conclude that $\sum_{p=1}^{\infty} \mathbb{P}_0^p(\bar{A}_p) < \infty$. Hence the proof. \square

A.2 Additional simulation results

Figures S1-S6 report the UMAP plots of the simulated datasets of Section 6. In each figure, the left column represents the true clustering and the right column the estimated Lamb clustering. Each figure's caption also specifies the true number of clusters (k_0) and the sample sizes (n).

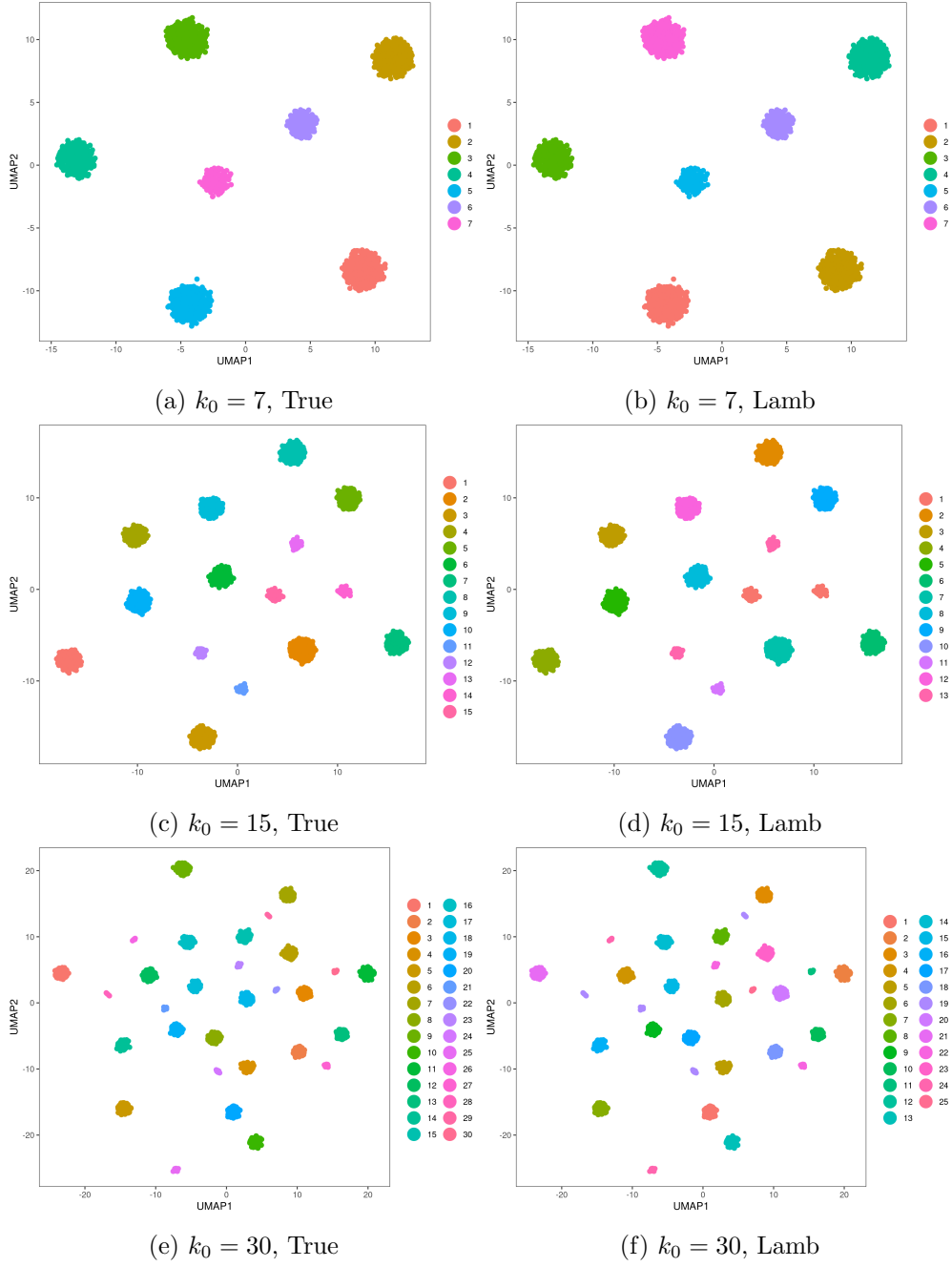


Figure S1: UMAP plots of simulated datasets from Scenario 1 and $n = 2500$.

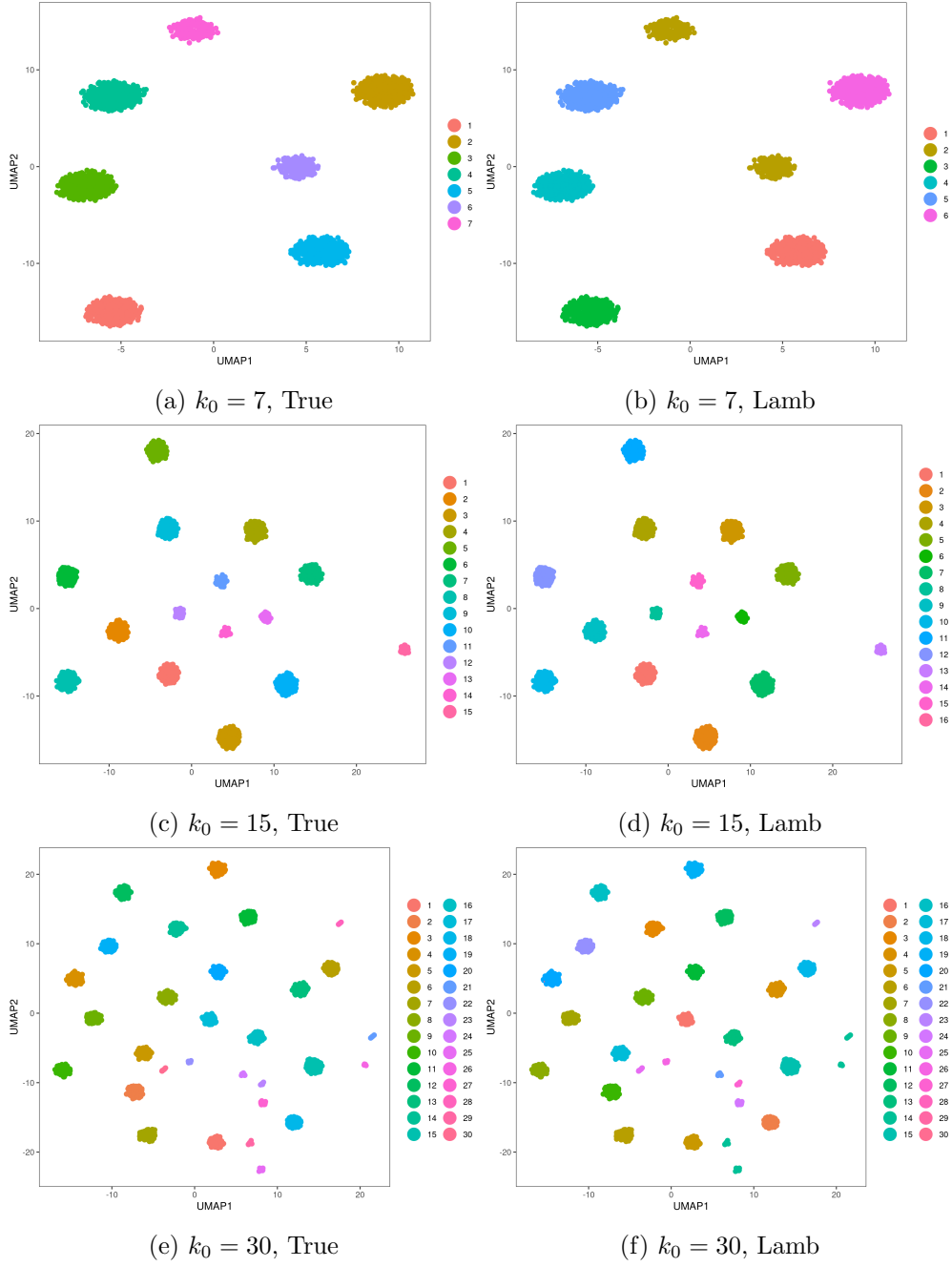


Figure S2: UMAP plots of simulated datasets from Scenario 1, and $n = 5000$.

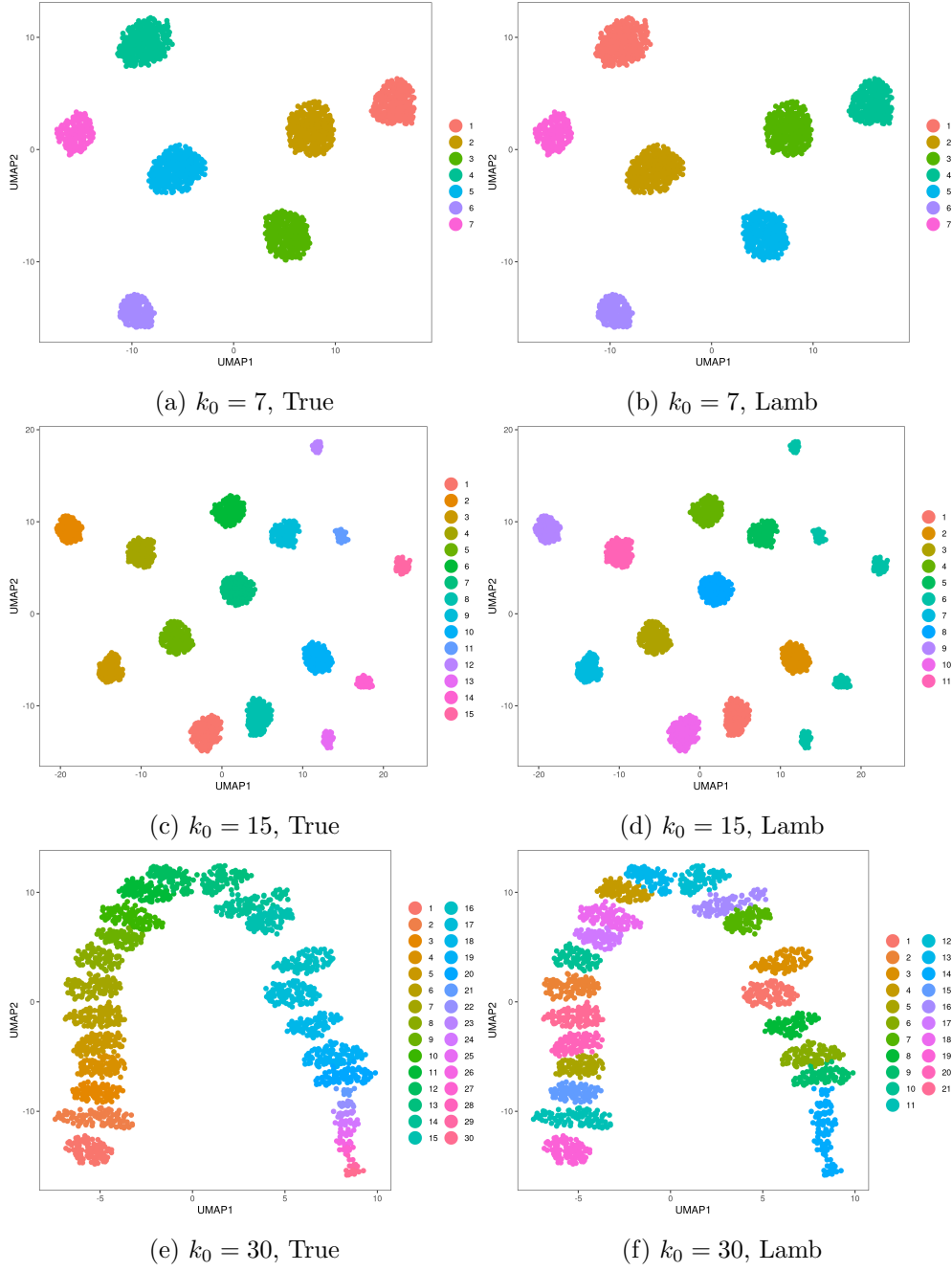
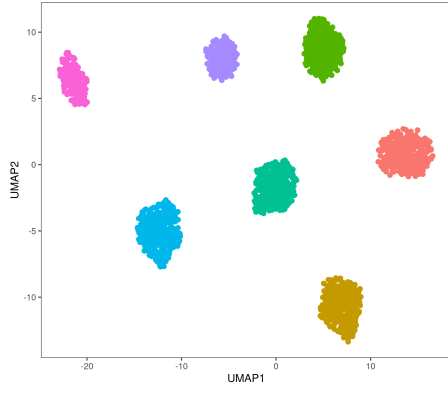
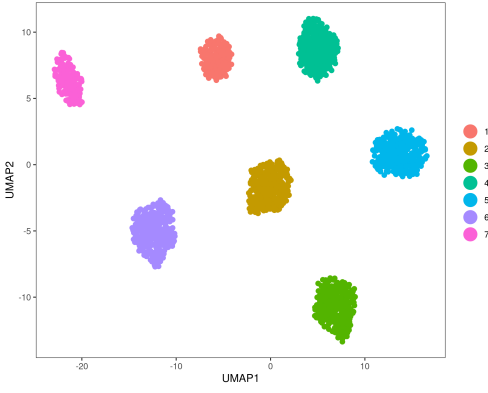


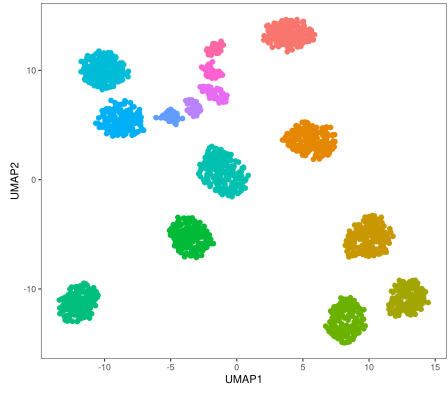
Figure S3: UMAP plots of simulated datasets from Scenario 2, and $n = 2500$.



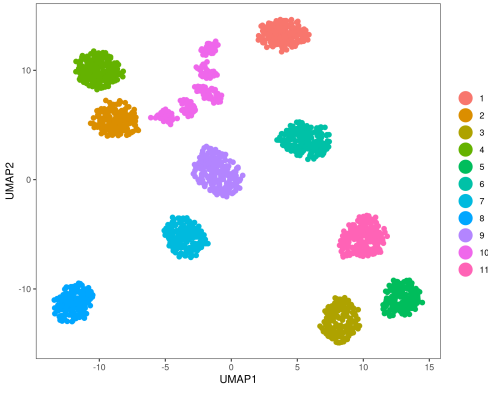
(a) $k_0 = 7$, True



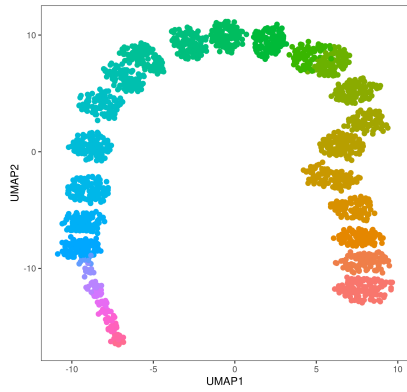
(b) $k_0 = 7$, Lamb



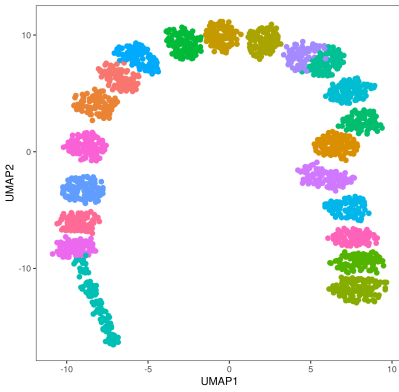
(c) $k_0 = 15$, True



(d) $k_0 = 15$, Lamb

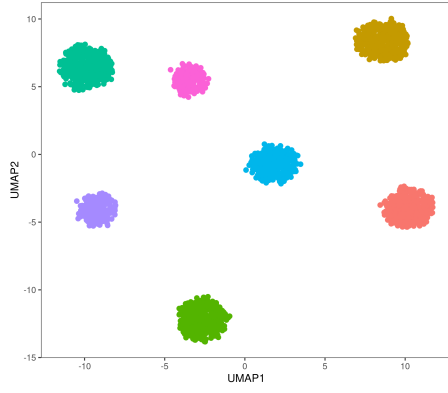


(e) $k_0 = 30$, True

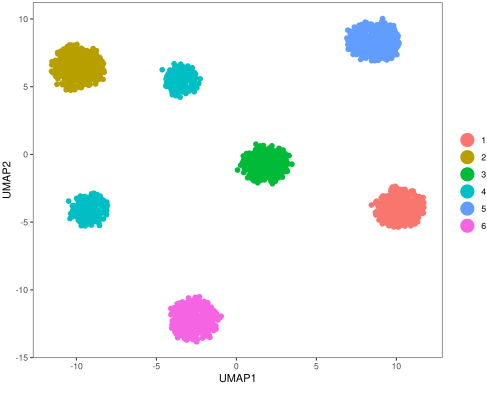


(f) $k_0 = 30$, Lamb

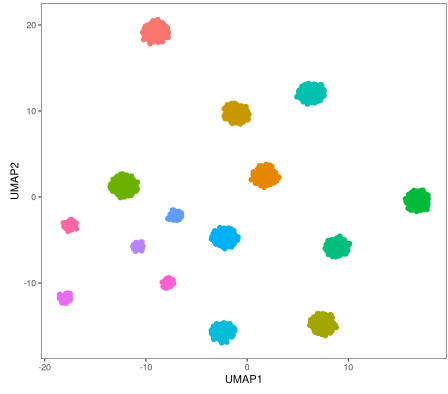
Figure S4: UMAP plots of simulated datasets from Scenario 2 and $n = 5000$



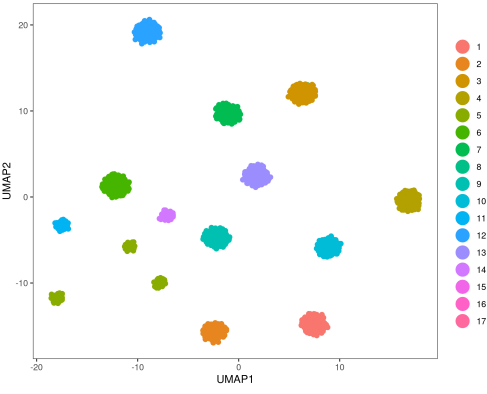
(a) $k_0 = 7$, True



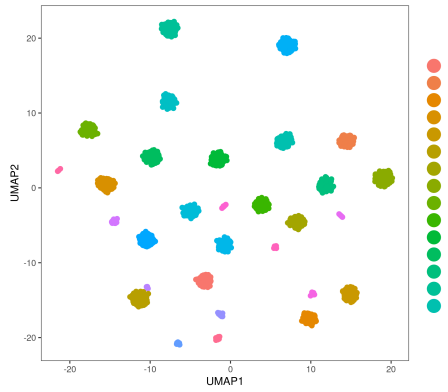
(b) $k_0 = 7$, Lamb



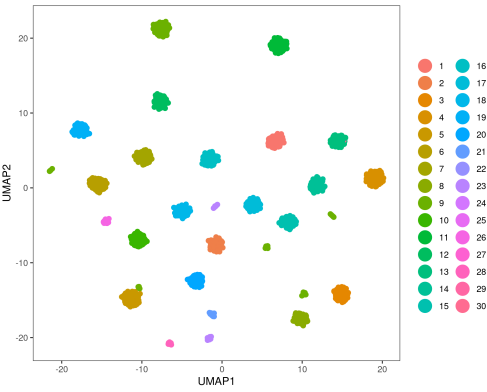
(c) $k_0 = 15$, True



(d) $k_0 = 15$, Lamb



(e) $k_0 = 30$, True



(f) $k_0 = 30$, Lamb

Figure S5: UMAP plots of simulated datasets from Scenario 3, and $n = 2500$.

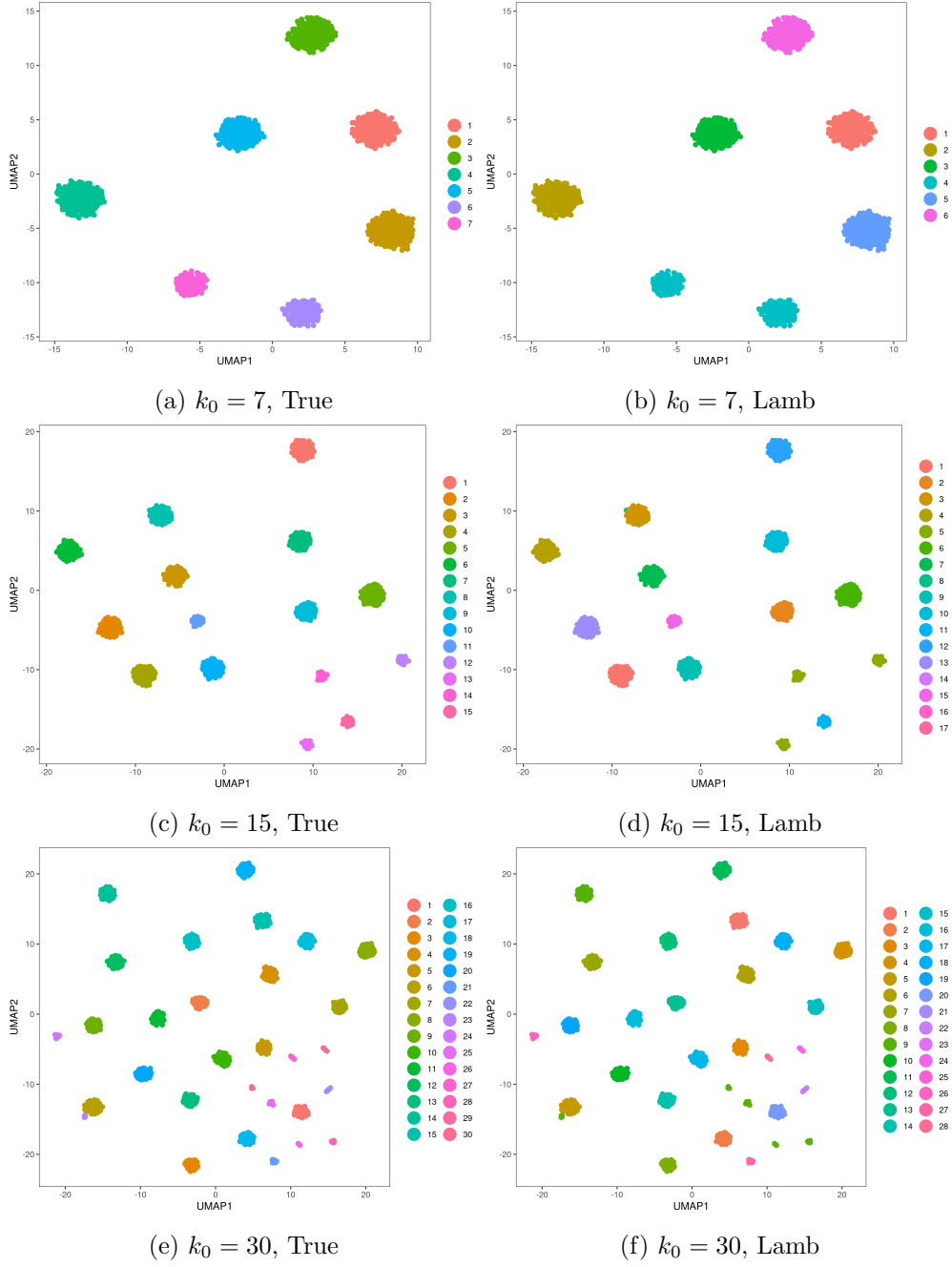


Figure S6: UMAP plots of simulated datasets from Scenario 3 and $n = 5000$